Available online at:
https://www.iasj.net/iasj?func=issueTOC&isId=9923&uiLanguage=ar

ISSN –1817 –2695

Received 14-10-2019, Accepted 6-11-2019

TIME DEPENDENT SPIN TRANSPORT THROUGH T – SHAPED DOUBLE QUANTUM DOTS EMBEDDED BETWEEN TWO (HALF – METALLIC ScC BULK) LEADS

MAGED A. NATTIQ[a,1], JENAN M. Al-MUKH[a], JABBAR M. KHALAF Al-ZYADI[a]

[a] Department of Physics, College of Education for Pure Sciences, University of Basrah, Iraq
E-mail: [1]majednatiq@gmil.com (Maged A. Nattiq)

ABSTRACT

For the experimental and theoretical importance of the time – dependent spin transport through quantum dots structures, the electromagnetic field–assisted spin transport through T–shaped double quantum dots embedded between two not normal leads are studied and analyzed. The time – dependent Hamiltonian, that describes the device, follows the tight binding scheme by taking all the spin dependent coupling interactions between the subsystems into consideration. The theoretical treatment is accomplished using the time – evolution operator approach, since the equations of motion in the interaction representation for the time – evolution operator matrix elements are derived. The thirty two intgro-differential equations of motion for both spin are solved numerically by using sixth order Runge Kutta method, since the error is checked in each step of time. The energy dependent calculations are achieved by considering the density of states of the not normal leads. While the adiabatic approximation is used to treat the effects of the external electromagnetic field characteristic (frequency and amplitude) theoretically. In concern to the not normal leads, the study concentrated the first-principles full-potential linearized augmented plane-wave method (FPLAPW), this method depends on the use of the density functional theory to examine the structural, magnetic, and electronic characteristics of the bulk of Zinc-blende ScC. This study has proven that both of the bulk ZB ScC is half- metallic ferromagnet at an equilibrium lattice constant of (0.5121 nm). The main goal of our study is to investigate the effects of the electromagnetic field on the T–shaped double quantum dots device, so all the electronic properties of the device as well as the electromagnetic field parameters are taken into consideration in our treatment. The role of the field frequency and the spin dependent coupling interaction are well analyzed and explained for the ScC bulk leads.

Keywords: *spintronics, magnetic nanostructure, half metallic density of states, time – dependent spin transport, time evolution operator technique.*

1- INTRODUCTION

The branch of nanotechnology (Nano-electronics) discusses integrated devices, information processing, nano scale electronic components and other new technologies. Recently, the basic physical effects can be investigated in a very controlled way due to the continuous development in nanofabrication, as an example for such controllable devices is the quantum dot devices [1-7]. The geometry of the quantum dots systems along with the physical parameters that can be adjusted in these systems allow directly the observation of these effects in electron (and spin) transport experiments. In double- quantum dot systems (DQDs), the component dots can be arranged in series, in parallel or in a T-shaped configuration [8-9]. In these configurations one or both quantum dots are connected to external leads depending on the configuration. Each of these arrangements has different physical properties that can be employed in new electronic and spintronics devices [10]. The T-shaped double QD (TDQD) system has been investigated both theoretically and experimentally [11,12], because there are two separate channels of spin transport which gives rise to many-particle effects and quantum interferences [13]. On the other side, hybrid resonant systems composed of one or more QDs coupled to normal-metal, ferromagnet and superconductor electrodes have been studied extensively [14]. In the T-shaped DQDs, only one central quantum dot connects to two leads via coupling tunneling interaction, while the other one is side coupled to the central one. The T-shape DQD system is a very promising QD configuration, both from the fundamental physics and possible applications in spintronics [15,16]. Recently, the time dependent quantum transport merit of quantum dot systems has considered a vital research area consequent for potential applications in nano-electronic devices. Application of external A.C. field on a quantum dot system leads to the time dependent quantum transport and one of the essential features is the well-known photon assisted tunneling [17,18]. Efficacious generation and monitoring of spin currents at the nanoscale is considered as a one of the central objectives of spin nano-electronics. This is due to highly spin –polarized currents that can be utilized to discover the spin state of a magnetic nano-structure, which is critical for applications in an information storage technologies [19],. However, the spin transport features with the interplay of the A.C. field and quantum interference in a T-shaped DQD device have not been fully studied. Therefore, our study aims to analyze and investigate the time – dependence of spin transport through T–shaped double quantum dots, coupled to half metallic ScC bulk leads, in presence of electromagnetic field. To arrive our aim, the time evolution of the T-shaped double quantum dots charge and spin currents flowing in the system are described in term of the time – evolution operator which is given by the equation of motion in the interaction representation. This extended theoretical treatment, which takes all the quantum interference effects into consideration, is invested to write program by Fotran language to calculate the time and spin dependence of the transport properties of the device.

In concern to the leads, the first-principles full-potential linearized augmented plane-wave method (FPLAPW), that depends on use of the density functional theory, is used to examine the structural, magnetic, and electronic characteristics of the bulk of ZB ScC. Which can be used as leads for the device considered in our study.

2- MODEL CALCULATION

In this paper we consider T- shaped double quantum dots. The quantum dot QD1 is embedded between two not normal leads while the second quantum dot QD2 is side coupled to the first one (see fig.1). In our treatment, we assume that the left and right electrodes are characterized by half-metallic leads. Two different density of states biased structures in each lead may break the spatial symmetry of the system. Form experimental point of view such study is important because in real nano-systems, the leads are often characterizes by nontrivial band structures i.e. band with peaks, surface states or gapes. So the lead's density of states plays a crucial role in the spin transport in nano-systems.

In our treatment we use the time evolution operator method which was successfully applied for time dependent of the external perturbations [27]. The problem we study is relatively complex because we take the following into consideration :

1- The time and spin dependent transport through the spin dependent tunneling barriers with not normal leads.
2- The presence of external electromagnetic field applied to subsystems including the time dependent of the quantum dots energy levels.
3- The equations of motion that must be solved are for both spin, neglecting the correlation energy on the subsystem as well as the spin flip in the structure.
4- The direct coupling interaction between the quantum dots is considered as a spin dependent one.
5- The spin dependent of the coupling interactions between the QD1 and the leads.
6- The spin dependent Fermi distribution function for the electrons in the not normal leads.
7- The temperature of the leads is fixed 0 K.

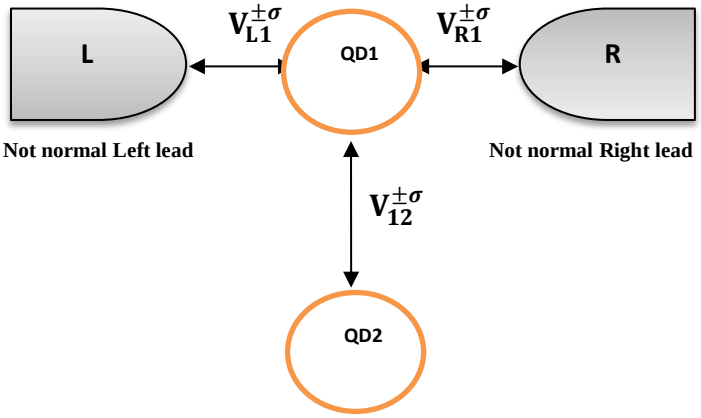

Fig. 1: Schematic illustration of the double quantum dots forming a T- shaped configuration between two not normal leads.

In order to describe the system considered in our study, we use the following Hamiltonian:

$$H(t) = H_o + V(t) \tag{1}$$

$$H_o = H_R + H_L + H_{D1} + H_{D2} \tag{2}$$

$$H_R = \sum_{k_R,\sigma} E_{k_R}^{\sigma}\, n_{k_R}^{\sigma}$$

$$H_L = \sum_{k_L,\sigma} E_{k_L}^{\sigma}\, n_{k_L}^{\sigma}$$

$$H_{D1} = \sum_{\sigma} E_1^{\sigma}\, n_1^{\sigma}$$

$$H_{D2} = \sum_{\sigma} E_2^{\sigma}\, n_2^{\sigma} \tag{3}$$

Where, $H_\alpha(\alpha = L, R)$ describe the right and left leads and $H_{Di}(i = 1,2)$ describe the double quantum dots. $E_{k_\alpha}^{\sigma}$ denote the energy levels of the leads and E_i^{σ} denote the energy levels of the quantum dots for certain spin σ. The occupation numbers $n_{k_\alpha}^{\sigma}$ and n_i^{σ} are given by :

$$n_{k_\alpha}^{\sigma} = C_{k_\alpha}^{\sigma+}\, C_{k_\alpha}^{\sigma}$$
$$n_i^{\sigma} = C_i^{\sigma+}\, C_i^{\sigma} \tag{4}$$

Where $C_i^{\sigma+}$ (C_i^{σ}) is the creation (annihilation) operator of the electrons with spin σ in the dot. $C_{k_\alpha}^{\sigma+}$ ($C_{k_\alpha}^{\sigma}$) is the creation (annihilation) operator of the electron with spin σ in the lead α.

The tunneling Hamiltonian can be given by,

$$V^{\sigma}(t) = V_{12}^{\sigma}(t)\, C_{1\sigma}^{+}(t)\, C_{2\sigma}(t) + V_{21}^{\sigma}(t)\, C_{2\sigma}^{+}(t)\, C_{1\sigma}(t) + \sum_{\alpha}\sum_{k_\alpha}\left[V_{1k_\alpha}^{\sigma}(t) C_{1\sigma}^{+}(t) C_{k_\alpha\sigma}(t) + V_{k_\alpha 1}^{\sigma}(t) C_{k_\alpha\sigma}^{+}(t) C_{1\sigma}(t)\right] \quad (5)$$

The tunneling coupling matrix elements between the central quantum dot and the leads are denoted by $V_{1k_\alpha}^{\sigma}$. While V_{12}^{σ} denotes the coupling interaction between the central quantum dot and the side coupled one.

The time evolution of the T-shaped DQD charge and current flowing in the system can be described in terms of the time- evolution operator $U(t, t_o)$ given by the equation of motion in the interaction representation (in atomic unit) [20,21],

$$i\,\frac{\partial U(t,t_o)}{\partial t} = \tilde{V}^{\sigma}(t) U(t, t_o) \quad (6)$$

where,

$$\tilde{V}^{\sigma}(t) = U_o(t, t_o)\, V^{\sigma}(t)\, U_o^{\dagger}(t, t_o) \quad (7)$$

It is assumed that the interaction between the subsystems are switched on the distant past t_o, and,

$$U_o(t, t_o) = e^{iH_o(t-t_o)} \quad (8)$$

Here H_o denotes the four terms of Eq.(2) and $V^{\sigma}(t)$ corresponds to all the other terms of the Hamiltonian defined in eq.(5). By substituting eq.(8) in eq.(7) we get,

$$\tilde{V}^{\sigma}(t) = e^{iH_o t}\, e^{-iH_o t_o}\, V^{\sigma}(t)\, e^{-iH_o t}\, e^{iH_o t_o} \quad (9)$$

Then, by substituting eq.(5) in eq.(9), we get,

$$\begin{aligned}\tilde{V}^{\sigma}(t) \quad & \tilde{V}_{12}^{\sigma}(t) C_{1\sigma}^{+}(t) C_{2\sigma}(t) \\ & + \tilde{V}_{21}^{\sigma}(t) C_{2\sigma}^{+}(t) C_{1\sigma} \\ & + \sum_{K_L}\left[\tilde{V}_{1K_L}^{\sigma}(t) C_{1\sigma}^{+}(t) C_{K_L\sigma}(t)\right. \\ & \left. + \tilde{V}_{K_L 1}^{\sigma}(t) C_{K_L\sigma}^{+}(t) C_{1\sigma}(t)\right] \\ & + \sum_{K_R}\left[\tilde{V}_{1K_R}^{\sigma}(t) C_{1\sigma}^{+}(t) C_{K_R\sigma}(t)\right. \\ & \left. + \tilde{V}_{K_R 1}^{\sigma}(t) C_{K_R\sigma}^{+}(t) C_{1\sigma}(t)\right] \end{aligned} \quad (10)$$

$\tilde{V}_{ij}{}^{\sigma}(t)$ are defined by,

$$\langle i\sigma|\tilde{V}(t)|j\sigma'\rangle = \delta_{\sigma\sigma'}\langle i\sigma|\tilde{V}^{\sigma}(t)|j\sigma\rangle \quad (11)$$

The electron occupancy of the main quantum dot $n_1^{\sigma}(t)$ and the side coupled quantum dot $n_2^{\sigma}(t)$with the spin σ, by using the time evolution operator technique, can be given in terms of the appropriate matrix elements of the evolution operator [21,22]:

$$\begin{aligned} n_1^{\sigma}(t) \quad & = n_1^{\sigma}(t_o)\left|U_{1\sigma,1\sigma}(t, t_o)\right|^2 \\ & + n_2^{\sigma}(t_o)\left|U_{1\sigma,2\sigma}(t, t_o)\right|^2 \\ & + \sum_{k_L} n_{k_L}^{\sigma}(t_o)\left|U_{1\sigma,k_L\sigma}(t, t_o)\right|^2 \\ & + \sum_{k_R} n_{k_R}^{\sigma}(t_o)\left|U_{1\sigma,k_R\sigma}(t, t_o)\right|^2 \end{aligned} \quad (12)$$

and,

$$\begin{aligned} n_2^{\sigma}(t) \quad & = n_2^{\sigma}(t_o)\left|U_{2\sigma,2\sigma}(t, t_o)\right|^2 \\ & + n_1^{\sigma}(t_o)\left|U_{2\sigma,1\sigma}(t, t_o)\right|^2 \\ & + \sum_{k_L} n_{k_L}^{\sigma}(t_o)\left|U_{2\sigma,k_L\sigma}(t, t_o)\right|^2 \end{aligned}$$

$$+\sum_{k_R} n^{\sigma}_{k_R}(t_o)\left|U_{2\sigma,k_R\sigma}(t,t_o)\right|^2 \qquad (13)$$

With $n^{\sigma}_1(t_o)$, $n^{\sigma}_2(t_o)$, $n^{\sigma}_{k_L}(t_o)$ and $n^{\sigma}_{k_R}(t_o)$ denote the initial occupancy of the main quantum dot, side coupled quantum dot, and left and right leads, respectively. $U_{i\sigma,j\sigma}(t,t_o)=\langle i\sigma|U(t,t_o)|j\sigma\rangle$ are the appropriate matrix elements of the operator $U(t,t_o)$. $|i\sigma\rangle$ and $|j\sigma\rangle$ belong to the operator of basis functions $\{|1\sigma\rangle, |2\sigma\rangle, |k_L\rangle$ and $|k_R\rangle\}$. The identity operator assumed to be,

$$\begin{aligned}\mathbf{I} &= \sum_{\sigma'=\sigma,-\sigma}[\,|\mathbf{1\sigma'}><\mathbf{1\sigma'}|\\ &+|\mathbf{2\sigma'}><\mathbf{2\sigma'}|\\ &+\sum_{\mathbf{k_L}}|\mathbf{k_L\sigma'}><\mathbf{k_L\sigma'}|\\ &+\sum_{\mathbf{k_R}}|\mathbf{k_R\sigma'}><\mathbf{k_R\sigma'}|]\end{aligned} \qquad \mathbf{(14)}$$

It follows from eq.(12) and eq.(13) that in order to calculate the occupation numbers $n^{\sigma}_1(t_o)$ and $n^{\sigma}_2(t_o)$ we have to calculate the matrix elements$U_{1\sigma,1\sigma}(t,t_0)$, $U_{1\sigma,2\sigma}(t,t_0)$, $U_{2\sigma,2\sigma}(t,t_0)$, $U_{2\sigma,1\sigma}(t,t_0)$, $U_{i\sigma,k_\alpha\sigma}(t,t_0)$ and $U_{k_\alpha\sigma,i\sigma}(t,t_0)$ with i=1,2 and $\alpha = L, R$. Now, in order to calculate $U_{1\sigma,1\sigma}(t,t_0)$ one should construct its equation of motion by writing,

$$i\frac{\partial}{\partial t}\langle 1\sigma|U(t,t_o)|1\sigma\rangle = \left\langle 1\sigma\middle|\tilde{V}^{\sigma}(t)U(t,t_o)\middle|1\sigma\right\rangle \qquad (15)$$

Then, after some algebra we get the following set of equations of motion for the required time evolution operators. The algebra that must be performed to derive the equations of motion for these time evolution operators matrix elements are presented in Tables (1-4).

Table (1) : The matrix elements $\langle 1\sigma|\tilde{V}^{\sigma}(t)|j\sigma\rangle$ *where* $j = 1\sigma, 2\sigma, k_L\sigma, k_R\sigma$

Bra \ Ket	$\|\mathbf{1\sigma}\rangle$	$\|\mathbf{2\sigma}\rangle$	$\sum_{\mathbf{k'_L}}\|\mathbf{k'_L\sigma}\rangle$	$\sum_{\mathbf{k'_R}}\|\mathbf{k'_R\sigma}\rangle$
$\langle \mathbf{1\sigma}\|\tilde{\mathbf{V}}^{\sigma}_{\mathbf{12}}(\mathbf{t})\ \mathbf{C}^{+}_{\mathbf{1\sigma}}(\mathbf{t})\mathbf{C}_{\mathbf{2\sigma}}(\mathbf{t})$	———	$\tilde{V}^{\sigma}_{12}(t)\langle 1\sigma\|1\sigma\rangle = \tilde{V}_{12}(t)$	———	———
$\langle \mathbf{1\sigma}\|\tilde{\mathbf{V}}^{\sigma}_{\mathbf{21}}(\mathbf{t})\ \mathbf{C}^{+}_{\mathbf{2\sigma}}(\mathbf{t})\mathbf{C}_{\mathbf{1\sigma}}(\mathbf{t})$	$\tilde{V}^{\sigma}_{21}(t)\langle 1\sigma\|2\sigma\rangle = 0$	———	———	———
$\langle \mathbf{1\sigma}\|\sum_{\mathbf{k_L}}\tilde{\mathbf{V}}^{\sigma}_{\mathbf{1K_L}}(\mathbf{t})\ \mathbf{C}^{+}_{\mathbf{1\sigma}}(\mathbf{t})\mathbf{C}_{\mathbf{k_L\sigma}}(\mathbf{t})$	———	———	$\sum_{K_L}\tilde{V}^{\sigma}_{1K_L}(t)\langle 1\sigma\|1\sigma\rangle = \sum_{K_L}\tilde{V}^{\sigma}_{1K_L}(t)$	———
$\langle \mathbf{1\sigma}\|\sum_{\mathbf{k_L}}\tilde{\mathbf{V}}^{\sigma}_{\mathbf{K_L1}}(\mathbf{t})\ \mathbf{C}^{+}_{\mathbf{k_L\sigma}}(\mathbf{t})\mathbf{C}_{\mathbf{1\sigma}}(\mathbf{t})$	$\sum_{K_L}\tilde{V}^{\sigma}_{K_L1}(t)\langle 1\sigma\|K_L\sigma\rangle = 0$	———	———	———
$\langle \mathbf{1\sigma}\|\sum_{\mathbf{k_R}}\tilde{\mathbf{V}}^{\sigma}_{\mathbf{1K_R}}(\mathbf{t})\ \mathbf{C}^{+}_{\mathbf{1\sigma}}(\mathbf{t})\mathbf{C}_{\mathbf{k_R\sigma}}(\mathbf{t})$	———	———	———	$\sum_{K_R}\tilde{V}^{\sigma}_{1K_R}(t)\langle 1\sigma\|1\sigma\rangle = \sum_{K_R}\tilde{V}^{\sigma}_{1K_R}(t)$
$\langle \mathbf{1\sigma}\|\sum_{\mathbf{k_R}}\tilde{\mathbf{V}}^{\sigma}_{\mathbf{K_R1}}(\mathbf{t})\ \mathbf{C}^{+}_{\mathbf{k_R\sigma}}(\mathbf{t})\mathbf{C}_{\mathbf{1\sigma}}(\mathbf{t})$	$\sum_{K_R}\tilde{V}^{\sigma}_{K_R1}(t)\langle 1\sigma\|K_R\sigma\rangle = 0$	———	———	———

Table (2) : The matrix elements $\langle 2\sigma|\tilde{V}^{\sigma}(t)|j\sigma\rangle$ *where* $j = 1\sigma, 2\sigma, k_L\sigma, k_R\sigma$

Bra \ Ket	$\|\mathbf{1\sigma}\rangle$	$\|\mathbf{2\sigma}\rangle$	$\sum_{\mathbf{k'_L}}\|\mathbf{k'_L\sigma}\rangle$	$\sum_{\mathbf{k'_R}}\|\mathbf{k'_R\sigma}\rangle$
$\langle \mathbf{2\sigma}\|\tilde{\mathbf{V}}^{\sigma}_{\mathbf{12}}(\mathbf{t})\ \mathbf{C}^{+}_{\mathbf{1\sigma}}(\mathbf{t})\mathbf{C}_{\mathbf{2\sigma}}(\mathbf{t})$	———	$\tilde{V}^{\sigma}_{12}(t)\langle 2\sigma\|1\sigma\rangle = 0$	———	———
$\langle \mathbf{2\sigma}\|\tilde{\mathbf{V}}^{\sigma}_{\mathbf{21}}(\mathbf{t})\ \mathbf{C}^{+}_{\mathbf{2\sigma}}(\mathbf{t})\mathbf{C}_{\mathbf{1\sigma}}(\mathbf{t})$	$\tilde{V}^{\sigma}_{21}(t)\langle 2\sigma\|2\sigma\rangle = \tilde{V}_{21}(t)$	———	———	———
$\langle \mathbf{2\sigma}\|\sum_{\mathbf{k_L}}\tilde{\mathbf{V}}^{\sigma}_{\mathbf{1K_L}}(\mathbf{t})\ \mathbf{C}^{+}_{\mathbf{1\sigma}}(\mathbf{t})\mathbf{C}_{\mathbf{k_L\sigma}}(\mathbf{t})$	———	———	$\sum_{K_L}\tilde{V}^{\sigma}_{1K_L}(t)\langle 2\sigma\|1\sigma\rangle = 0$	———
$\langle \mathbf{2\sigma}\|\sum_{\mathbf{k_L}}\tilde{\mathbf{V}}^{\sigma}_{\mathbf{K_L1}}(\mathbf{t})\ \mathbf{C}^{+}_{\mathbf{k_L\sigma}}(\mathbf{t})\mathbf{C}_{\mathbf{1\sigma}}(\mathbf{t})$	$\sum_{K_L}\tilde{V}^{\sigma}_{K_L1}(t)\langle 2\sigma\|K_L\sigma\rangle = 0$	———	———	———
$\langle \mathbf{2\sigma}\|\sum_{\mathbf{k_R}}\tilde{\mathbf{V}}^{\sigma}_{\mathbf{1K_R}}(\mathbf{t})\ \mathbf{C}^{+}_{\mathbf{1\sigma}}(\mathbf{t})\mathbf{C}_{\mathbf{k_R\sigma}}(\mathbf{t})$	———	———	———	$\sum_{K_R}\tilde{V}^{\sigma}_{1K_R}(t)\langle 2\sigma\|1\sigma\rangle = 0$
$\langle \mathbf{2\sigma}\|\sum_{\mathbf{k_R}}\tilde{\mathbf{V}}^{\sigma}_{\mathbf{K_R1}}(\mathbf{t})\ \mathbf{C}^{+}_{\mathbf{k_R\sigma}}(\mathbf{t})\mathbf{C}_{\mathbf{1\sigma}}(\mathbf{t})$	$\sum_{K_R}\tilde{V}^{\sigma}_{K_R1}(t)\langle 2\sigma\|K_R\sigma\rangle = 0$	———	———	———

Table (3): The matrix elements $\langle k_L''\sigma|\tilde{V}^{\sigma}(t)|j\sigma\rangle$ *where* $j = 1\sigma, 2\sigma, k_L\sigma, k_R\sigma$

Bra \ Ket	$\|1\sigma\rangle$	$\|2\sigma\rangle$	$\sum_{k_L'}\|k_L'\sigma\rangle$	$\sum_{k_R'}\|k_R'\sigma\rangle$
$\langle k_L''\sigma\|\tilde{V}_{12}^{\sigma}(t)\ C_{1\sigma}^{+}(t)C_{2\sigma}(t)$	____	$\tilde{V}_{12}^{\sigma}(t)\langle K_L''\sigma\|1\sigma\rangle = 0$	____	____
$\langle k_L''\sigma\|\tilde{V}_{21}^{\sigma}(t)\ C_{2\sigma}^{+}(t)C_{1\sigma}(t)$	$V_{21}^{\sigma}(t)\langle K_L''\sigma\|2\sigma\rangle = 0$	____	____	____
$\langle k_L''\sigma\|\sum_{k_L}\tilde{V}_{1K_L}^{\sigma}(t)\ C_{1\sigma}^{+}(t)C_{k_L\sigma}(t)$	____	____	$\sum_{K_L}\tilde{V}_{1K_L}^{\sigma}(t)\langle K_L''\sigma\|1\sigma\rangle = 0$	____
$\langle k_L''\sigma\|\sum_{k_L}\tilde{V}_{K_L1}^{\sigma}(t)\ C_{k_L\sigma}^{+}(t)C_{1\sigma}(t)$	$\sum_{K_L}\tilde{V}_{K_L1}^{\sigma}(t)\langle K_L''\sigma\|K_L\sigma\rangle = \tilde{V}_{K_L''1}^{\sigma}(t)$	____	____	____
$\langle k_L''\sigma\|\sum_{k_R}\tilde{V}_{1K_R}^{\sigma}(t)\ C_{1\sigma}^{+}(t)C_{k_R\sigma}(t)$	____	____	____	$\sum_{K_R}\tilde{V}_{1K_R}^{\sigma}(t)\langle K_L''\sigma\|1\sigma\rangle = 0$
$\langle k_L''\sigma\|\sum_{k_R}\tilde{V}_{K_R1}^{\sigma}(t)\ C_{k_R\sigma}^{+}(t)C_{1\sigma}(t)$	$\sum_{K_R}\tilde{V}_{K_R1}^{\sigma}(t)\langle K_L''\sigma\|K_R\sigma\rangle = 0$	____	____	____

Then, in order to incorporate the electronic

Table (4) : The matrix elements $\langle k_R''\sigma|\tilde{V}^{\sigma}(t)|j\sigma\rangle$ *where* $j = 1\sigma, 2\sigma, k_L\sigma, k_R\sigma$

Bra \ Ket	$\|1\sigma\rangle$	$\|2\sigma\rangle$	$\sum_{k_L'}\|k_L'\sigma\rangle$	$\sum_{k_R'}\|k_R'\sigma\rangle$
$\langle k_R''\sigma\|\tilde{V}_{12}^{\sigma}(t)\ C_{1\sigma}^{+}(t)C_{2\sigma}(t)$	____	$\tilde{V}_{12}^{\sigma}(t)\langle K_R''\sigma\|1\sigma\rangle = 0$	____	____
$\langle k_R''\sigma\|\tilde{V}_{21}^{\sigma}(t)\ C_{2\sigma}^{+}(t)C_{1\sigma}(t)$	$\tilde{V}_{21}^{\sigma}(t)\langle K_R''\sigma\|2\sigma\rangle = 0$	____	____	____
$\langle k_R''\sigma\|\sum_{k_L}\tilde{V}_{1K_L}^{\sigma}(t)\ C_{1\sigma}^{+}(t)C_{k_L\sigma}(t)$	____	____	$\sum_{K_L}\tilde{V}_{1K_L}^{\sigma}(t)\langle K_R''\sigma\|1\sigma\rangle = 0$	____
$\langle k_R''\sigma\|\sum_{k_L}\tilde{V}_{K_L1}^{\sigma}(t)\ C_{k_L\sigma}^{+}(t)C_{1\sigma}(t)$	$\sum_{K_L}\tilde{V}_{K_L1}^{\sigma}(t)\langle K_R''\sigma\|K_L\sigma\rangle = 0$	____	____	____
$\langle k_R''\sigma\|\sum_{k_R}\tilde{V}_{1K_R}^{\sigma}(t)\ C_{1\sigma}^{+}(t)C_{k_R\sigma}(t)$	____	____	____	$\sum_{K_R}\tilde{V}_{K_R1}^{\sigma}(t)\langle K_R''\sigma\|1\sigma\rangle = 0$
$\langle k_R''\sigma\|\sum_{k_R}\tilde{V}_{K_R1}^{\sigma}(t)\ C_{k_R\sigma}^{+}(t)C_{1\sigma}(t)$	$\sum_{K_R}\tilde{V}_{K_R1}^{\sigma}(t)\langle K_R''\sigma\|K_R\sigma\rangle = \tilde{V}_{K_R''1}^{\sigma}(t)$	____	____	____

properties of the leads, we introduce the following definitions, [23],

$$\tilde{V}_{iK_\alpha}^{\sigma}(t) = \upsilon_{K_\alpha}^{\sigma}\, V_{i\alpha}^{\sigma}(t)$$

$$\tilde{V}^{\sigma}_{K_\alpha i}(t) = \upsilon^{*\sigma}_{K_\alpha} V^{\sigma}_{\alpha i}(t) \qquad (16)$$

And

$$U_{k_\alpha\sigma,i\sigma}(t,t_o) = \upsilon^{*\sigma}_{K_\alpha} U_{\alpha\sigma,i\sigma}(t,t_o)$$

$$U_{i\sigma,k_\alpha\sigma}(t,t_o) = \upsilon^{\sigma}_{K_\alpha} U_{i\sigma,\alpha\sigma}(t,t_o) \qquad (17)$$

And,

$$U_{k_L\sigma,k_R\sigma}(t,t_o) = \upsilon^{*\sigma}_{K_L}\, \upsilon^{*\sigma}_{K_R} U_{L\sigma,R\sigma}(t,t_o) \qquad (18)$$

The general formula of the lead density of states is given by [24],

$$\rho^{\sigma}_{\alpha}(E^{\sigma}) = \sum_{k_\alpha} \left|\upsilon^{\sigma}_{K_\alpha}\right|^2 \delta\left(E - E^{\sigma}_{k_\alpha}\right) \qquad (19)$$

with [25],

$$1 = \int_{-\infty}^{+\infty} \delta\left(E - E^{\sigma}_{K_\alpha}\right) dE \qquad (20)$$

By substituting the above mentioned relations in the set of equations of motion, we get,

$$\begin{aligned} i\frac{\partial}{\partial t} U_{1\sigma,1\sigma}(t,t_o) &= V^{\sigma}_{12}(t) U_{1\sigma,1\sigma}(t,t_o) \\ &+ \int_{-\infty}^{+\infty} \rho^{\sigma}_{L}(E^{\sigma}_{L}) V^{\sigma}_{1L}(t) U_{L\sigma,1\sigma}(t,t_o) dE^{\sigma}_{L} \\ &+ \int_{-\infty}^{+\infty} \rho^{\sigma}_{R}(E^{\sigma}_{R})\, V^{\sigma}_{1R}(t) U_{R\sigma,1\sigma}(t,t_o) dE^{\sigma}_{R} \qquad (21) \end{aligned}$$

$$\begin{aligned} i\frac{\partial}{\partial t} U_{1\sigma,2\sigma}(t,t_o) &= V^{\sigma}_{12}(t) U_{2\sigma,2\sigma}(t,t_o) \\ &+ \int_{-\infty}^{+\infty} \rho^{\sigma}_{L}(E^{\sigma}_{L}) V^{\sigma}_{1L}(t) U_{L\sigma,2\sigma}(t,t_o) dE^{\sigma}_{L} \\ &+ \int_{-\infty}^{+\infty} \rho^{\sigma}_{R}(E^{\sigma}_{R})\, V^{\sigma}_{1R}(t) U_{R\sigma,2\sigma}(t,t_o) dE^{\sigma}_{R} \qquad (22) \end{aligned}$$

$$\begin{aligned} i\frac{\partial}{\partial t} U_{1\sigma,L'\sigma}(t,t_o) &= V^{\sigma}_{12}(t) U_{2\sigma,L'\sigma}(t,t_o) \\ &+ \int_{-\infty}^{+\infty} \rho^{\sigma}_{L}(E^{\sigma}_{L}) V^{\sigma}_{1L}(t) U_{L\sigma,L'\sigma}(t,t_o) dE^{\sigma}_{L} \\ &+ \int_{-\infty}^{+\infty} \rho^{\sigma}_{R}(E^{\sigma}_{R})\, V^{\sigma}_{1R}(t) U_{R\sigma,L'\sigma}(t,t_o) dE^{\sigma}_{R} \qquad (23) \end{aligned}$$

$$\begin{aligned} i\frac{\partial}{\partial t} U_{1\sigma,R'\sigma}(t,t_o) &= V^{\sigma}_{12}(t) U_{2\sigma,R'\sigma}(t,t_o) \\ &+ \int_{-\infty}^{+\infty} \rho^{\sigma}_{L}(E^{\sigma}_{L}) V^{\sigma}_{1L}(t) U_{L\sigma,R'\sigma}(t,t_o) dE^{\sigma}_{L} \\ &+ \int_{-\infty}^{+\infty} \rho^{\sigma}_{R}(E^{\sigma}_{R})\, V^{\sigma}_{1R}(t) U_{R\sigma,R'\sigma}(t,t_o) dE^{\sigma}_{R} \qquad (24) \end{aligned}$$

$$i\frac{\partial}{\partial t}U_{2\sigma,2\sigma}(t,t_o) = V_{21}^{\sigma}(t)U_{1\sigma,2\sigma}(t,t_o) \quad (25)$$

$$i\frac{\partial}{\partial t}U_{2\sigma,1\sigma}(t,t_o) = V_{21}^{\sigma}(t)U_{1\sigma,1\sigma}(t,t_o) \quad (26)$$

$$i\frac{\partial}{\partial t}U_{L\sigma,1\sigma}(t,t_o) = V_{L1}^{\sigma}(t)U_{1\sigma,1\sigma}(t,t_o) \quad (27)$$

$$i\frac{\partial}{\partial t}U_{R\sigma,1\sigma}(t,t_o) = V_{R1}^{\sigma}(t)U_{1\sigma,1\sigma}(t,t_o) \quad (28)$$

$$i\frac{\partial}{\partial t}U_{L\sigma,2\sigma}(t,t_o) = V_{L1}^{\sigma}(t)U_{1\sigma,2\sigma}(t,t_o) \quad (29)$$

$$i\frac{\partial}{\partial t}U_{R\sigma,2\sigma}(t,t_o) = V_{R1}^{\sigma}(t)U_{1\sigma,2\sigma}(t,t_o) \quad (30)$$

$$i\frac{\partial}{\partial t}U_{2\sigma,L\sigma}(t,t_o) = V_{21}(t)U_{1\sigma,L\sigma}(t,t_o) \quad (31)$$

$$i\frac{\partial}{\partial t}U_{2\sigma,R\sigma}(t,t_o) = V_{21}(t)U_{1\sigma,R\sigma}(t,t_o) \quad (32)$$

$$i\frac{\partial}{\partial t}U_{L'\sigma,L\sigma}(t,t_o) = V_{L'1}^{\sigma}(t)U_{1\sigma,L\sigma}(t,t_o) \quad (33)$$

$$i\frac{\partial}{\partial t}U_{R'\sigma,R\sigma}(t,t_o) = V_{R'1}^{\sigma}(t)U_{1\sigma,R\sigma}(t,t_o) \quad (34)$$

$$i\frac{\partial}{\partial t}U_{R\sigma,L\sigma}(t,t_o) = V_{R1}^{\sigma}(t)U_{1\sigma,L\sigma}(t,t_o) \quad (35)$$

$$i\frac{\partial}{\partial t}U_{L\sigma,R\sigma}(t,t_o) = V_{L1}^{\sigma}(t)U_{1\sigma,R\sigma}(t,t_o) \quad (36)$$

The knowledge of the matrix elements $U_{i\sigma,j\sigma}(t,t_o)$ is sufficient to calculate both the charge localized on each quantum dot and the electric current flowing through the system under consideration. In order to simplify the calculation of the occupation number, we introduce the following definition:,

$$C_{k_\alpha}^{\sigma}(t_o) \approx \sqrt{f_{\alpha}^{\sigma}(E_{k_\alpha}^{\sigma},T)} \quad (37)$$

$$n_{k_\alpha}^{\sigma} \approx f_{\alpha}^{\sigma}(E_{k_\alpha}^{\sigma},T) \quad (38)$$

Where $f_{\alpha}^{\sigma}(E_{k_\alpha}^{\sigma},T)$ is the spin dependent Fermi distribution function in the lead α, μ_α is the bias voltage that applied to the lead α, T is the temperature of the leads.

$$f_{k}^{\sigma}(E_{k}^{\sigma},T) = \frac{1}{1+\mathrm{Exp}(\frac{E_{k}^{\sigma}-\mu_k}{k_B T})} \quad (39)$$

By getting use of eq.(19) and (20), we get the following form:

$$n_1^{\sigma}(t) = n_1^{\sigma}(t_o)\left|U_{1\sigma,1\sigma}(t,t_o)\right|^2 + n_2^{\sigma}(t_o)\left|U_{1\sigma,2\sigma}(t,t_o)\right|^2 + \int dE_L^{\sigma}\ \rho_L^{\sigma}(E_L^{\sigma})\ f_L^{\sigma}(E_L^{\sigma},T)\left|U_{1\sigma,L\sigma}(t,t_o)\right|^2 + \int dE_R^{\sigma}\ \rho_R^{\sigma}(E_R^{\sigma})\ f_R^{\sigma}(E_R^{\sigma},T)\left|U_{1\sigma,R\sigma}(t,t_o)\right|^2 \quad (40)$$

and,

$$n_2^{\sigma}(t) = n_2^{\sigma}(t_o)\left|U_{2\sigma,2\sigma}(t,t_o)\right|^2 + n_1^{\sigma}(t_o)\left|U_{2\sigma,1\sigma}(t,t_o)\right|^2 + \int dE_L^{\sigma}\ \rho_L^{\sigma}(E_L^{\sigma})\ f_L^{\sigma}(E_L^{\sigma},T)\left|U_{2\sigma,L\sigma}(t,t_o)\right|^2 + \int dE_R^{\sigma}\ \rho_R^{\sigma}(E_R^{\sigma})\ f_R^{\sigma}(E_R^{\sigma},T)\left|U_{2\sigma,R\sigma}(t,t_o)\right|^2 \quad (41)$$

The tunneling current flowing from the left lead $I_L(t)$ can be obtained by using the time derivative of the total number of electrons in the left lead n_L^{σ} [26],

$$I^{\sigma} = -e\frac{dn_L^{\sigma}}{dt} \quad (42)$$

$$n_L^{\sigma}(t) = \iint dE_L^{\sigma}\ dE_{L'}^{\sigma}\ f^{\sigma}(E_{L'}^{\sigma},T)\rho_L^{\sigma}(E_L^{\sigma})\ \rho_{L'}^{\sigma}(E_{L'}^{\sigma})\ \left|U_{L\sigma,L'\sigma}(t,t_o)\right|^2 + \iint dE_L^{\sigma}\ dE_R^{\sigma} f^{\sigma}(E_R^{\sigma},T)\rho_L^{\sigma}(E_L^{\sigma})\ \rho_R^{\sigma}(E_R^{\sigma})\ \left|U_{L\sigma,R\sigma}(t,t_o)\right|^2$$

$$+\int dE_L^{\sigma}\, n_1^{\sigma}(t_o)\, \rho_L^{\sigma}(E_L^{\sigma})\, \left|U_{L\sigma,1\sigma}(t,t_o)\right|^2$$
$$+\int dE_L^{\sigma}\, n_2^{\sigma}(t_o)\, \rho_L^{\sigma}(E_L^{\sigma})\, \left|U_{L\sigma,2\sigma}(t,t_o)\right|^2$$

(43)

Which means that the spin dependent levels of the leads and the quantum dots are driven by the time dependent field with the frequency ω and the amplitudes Δ_α and Δ_i, respectively [27].

The static energy of the level E_{di}^{σ} depends on the D.C. gate voltage [28].

Therefore, our treatment is concerned with the elastic current in which electrons emit or absorb photons as a virtual process [29]. So, accordingly the dependent coupling interactions between the subsystem due to electromagnetic field is given by [30].

$$\widetilde{V}_{ij}^{\sigma}(t) = V_{ij}^{\sigma}\exp(i(E_i^{\sigma} - E_j^{\sigma})(t-t_o))\, \exp\left(i\,\frac{\Delta_i-\Delta_j}{\omega}\,(\sin(\omega t)-\sin(\omega t_o))\right)$$
$$i,j = 1,2,k_L,k_R \qquad (44)$$

Finally, as the leads considered in our treatment are not normal, extended theoretical treatment will be presented in section three to introduce the method used to calculate the density of states of the leads.

3- First-principles Study on the Half-metallic Ferromagnetism of Zinc-blende Structural ScC

The first-principles calculations based on the density functional theory accomplished in the Wien 2K code were applied to examine the magnetic and electronic characteristic of the bulk ScC at the expected equilibrium lattice constant of 0.5121 nm. The meshes used for the bulk ScC was 12 × 12 × 12 k meshes. Furthermore, the expansion was set up to be I= 10 and $R_{mt} \times K_{max}$ was equal to 8.0 in the muffin tins. In this study, the spin-orbital coupling was neglected since it has a trivial effect on the main findings. The radii R_{mt} of the muffin tins spheres in respective have set to 2.21 a.u. 1.96 a.u. of Sc and C atoms for the bulk. The self-correspondence of the overall energy variation between succeeding repetitions has been accomplished with a precision less than 10^{-5} Ry per formula unit. This project has focused on the geometry developments of the lattice steady of bulk ScC, by applying the ferromagnetic measurements of respective total energy vs lattice constant curve, as shown in Fig. 2. Therefore, the equilibrium lattice constant has been acquired from the smallest energy. Results was showed that the measured equilibrium lattice constant of bulk ScC is 0.5121 nm. Although there are no available experimental data to compare our findings with studies on FM HM of ZB TM pnictides, and chalcogenides have revealed that the ZB structure have no lowest total energy when compared with other crystal lattices. Nevertheless, the ZB films of CrAs and CrSb were manufactured from suitable ZB semiconducting materials [31]. The calculated total magnetic moment, the magnetic moments of the Sc, C and ScC have been awarded as a function of the lattice constant as represented in Fig. 3. It is clear that the bulk has ScC total magnetic moment amounting to 1 μ_B per formula unit; this value agrees with results of Reference [32].

The calculated total magnetic moment follows the Slater-Paulig law of the binary materials [33]:

$$M_{tot}=(Z_{tot}-8)\ \mu_B \qquad (45)$$

Where M_{tot} represents the total magnetic moment per formula unit and the Z_{tot} denotes the total number of valence electrons. In ZB ScC, the valence band contains seven electrons (Sc: $4s^2$, $3d^1$), (C: $2s^2$, $2p^2$), Thus, the number of electrons in each shell is equal to 7 and this implies that the total magnetic moments are equal to 1μ_B per formula unit which is the integer value. The integer value is considered one of the most important conditions and requirements of substances to be HM ferromagnetic. total magnetic moment of ScC consists two sections. The firstly is the total magnetic moment of the Sc atom (0.13479 μ_B), and the second is the C atom

(0.63758 μ_B). Thus it is the major participation to the total spin magnetic moment of ZB ScC which happens due to the spin polarization of C cases.

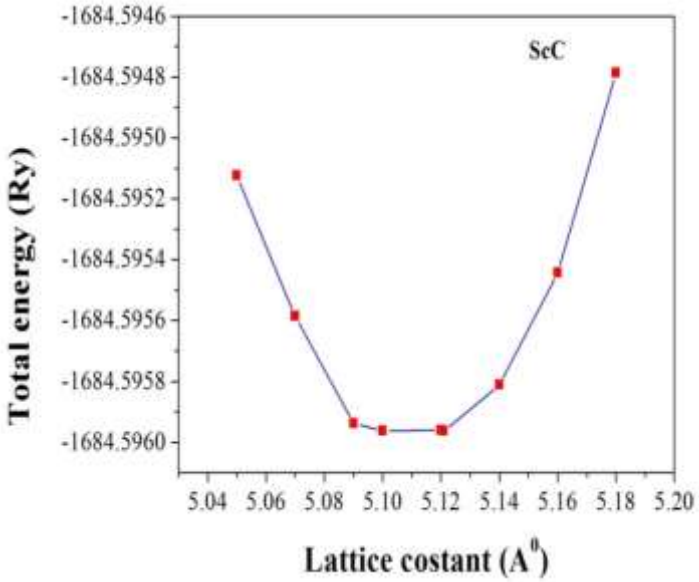

Fig. 2 Calculated total energy of the ScC as a function of lattice constant

under the Fermi level, while the s-state C is positioned about -8 eV below the Fermi level and do not appear in the figure above. The Fermi level has been set to zero and the spin located down was factored by -1. Moreover, it can be seen clearly from Fig.4 that there are energy gaps for the majority spin bands at the Fermi level in two components. The minority spin channel exhibits metal properties, analogous to the HM of compounds like ZB MnC, MC (M=Ca,Sr, and Ba), CaSi, and CaGe [34]. Thus, ScX materials are considered HM ferromagnets. In addition, one can see the presence of the HM gap [35] which can be known as the smallest value between the smallest energy of majority spin and minority spin conduction bands relating to the Fermi level. For the ScC compound, the HM gap is few, and it is placed in the midst of a gapless of semiconductor and the energy gap was 1.76 eV. These gaps are considered comparatively small when compared with those of other ZB HM compounds. However, it can lead to an increase in Curie temperatures, as it happened with other ZB HM compounds [34].

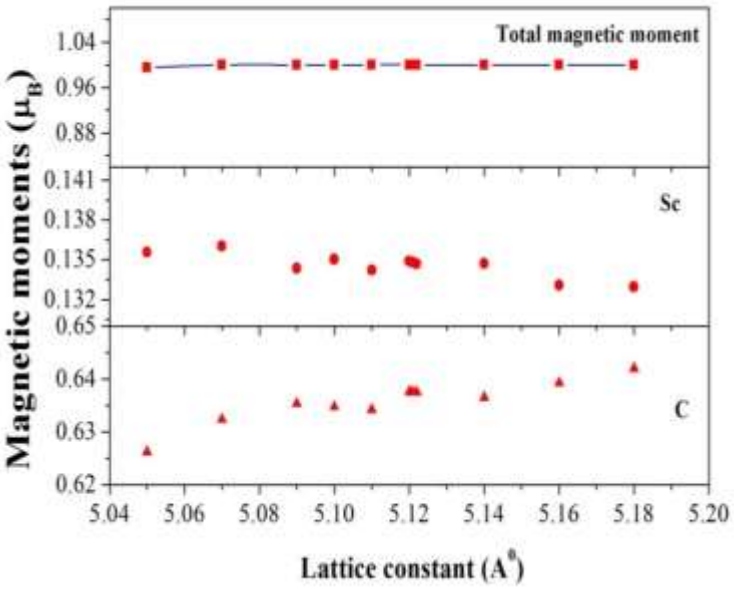

Fig.3 : The calculated total and partial magnetic moments (μ_B) for ScC

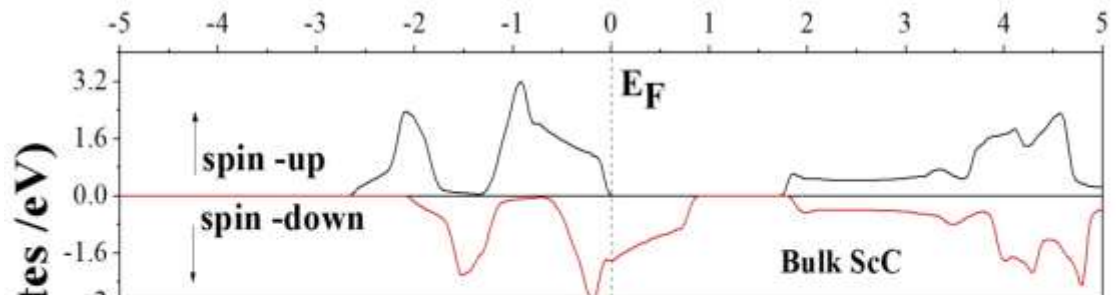

4- RESULTS AND DISCUSSIONS

We believe that the procedure presented in section two is reliable in the qualitative discussing of the physics of the spin transport through the considered system. We have derived 32 equations for the time and spin dependent time evolution operators that describe the device. The related set of integro- differential equations are solved numerically by using six order Runge – Kutta method where the error is checked at each time step with $\Delta t = 0.1\, a.u.$ The program language used is Fortran 90. The integration over energy is achieved by using Simpson method with ΔE is determined according to the leads density of states calculations that presented in section three, while the leads temperature is fixed at 0 K. For the case of biased leads, it is assumed that $\mu_L = -\mu_R$, where $\mu_L(\mu_R)$ is the chemical potential of the left (right) lead. The spin dependent quantum dots energy levels are determined by the following: $E_1^{\sigma} = E_2^{\sigma} = -0.5$ eV and $E_1^{-\sigma} = E_2^{-\sigma} = 0.5$ eV. This may be controlled by the effect of magnetic field (i. e Zeeman splitting). The dots used in our treatment is symmetric. The external electromagnetic field parameters are as follows: $\hbar\omega = 0.1$ eV, $\Delta_1 = 4$eV, $\Delta_2 = 1$ eV, $\Delta_L = 3$ eV, $\Delta_R = 0$. At the initial time t=t_0 = 0.0, the occupation numbers of the quantum dots n_i^{σ} (i = 1,2) are fixed at 0.5. We also assume that the coupling interactions between the subsystems are spin dependent with $V_{1\alpha}^{\sigma} = 0.15$ eV, $V_{1\alpha}^{-\sigma} = 0.05$ eV, $V_{12}^{\sigma} = 0.2$ eV, $V_{12}^{-\sigma} = 0.1$ eV.

Accordingly, it is easy to compute the occupation numbers of both quantum dots, the occupation number on the left lead and the current flowing through the device (calculated in atomic unit).

The parameters concerned to the external electromagnetic field are presented in each figure where $\Delta_1 > \Delta_2$ and $\Delta_L > \Delta_R$. The right lead is not affected by the external field, i.e $\Delta_R = 0$. In fig. (5), $n_i^{\pm\sigma}$ show oscillatory behavior with time, for t < 350 a.u. $n_1^{\pm\sigma}$ $(n_2^{\pm\sigma})$ decrease (increase) with time. For all times, it is noticed that $n_i^{-\sigma} > n_i^{+\sigma}$ except for t > 500 a.u. $n_2^{+\sigma}$ becomes larger than $n_2^{-\sigma}$. These results are physically accepted if we keep in mind that $V_{1\alpha}^{+\sigma} > V_{1\alpha}^{-\sigma}$ and $V_{12}^{+\sigma} > V_{12}^{-\sigma}$, this makes the time evolution of the states on QD1 (and QD2) for spin down greater than that of the spin up. The case for the occupation number on the left lead is different. For all time, it is obvious that $n_L^{+\sigma} \approx 0.5$ and $n_L^{-\sigma} \approx 0.4$, i.e. $n_L^{+\sigma} > n_L^{-\sigma}$. This does not contradict with our above mentioned

physical explanations about the time evolution of the spin up and spin down states. The spin current channels $I_L^{+\sigma}$ and $I_L^{-\sigma}$ flowing from the left lead show also oscillatory behavior keeping in mind that $\Delta_R = 0$. The spin currents are nearly vanished for t > 350 a.u.

The case of $V_{1\alpha}^{-\sigma} > V_{1\alpha}^{+\sigma}$ and $V_{12}^{-\sigma} > V_{12}^{+\sigma}$ is also studied and investigated (see Fig. 6)). The same above mentioned physical notes can be reported except for the occupation number on the left lead. It also be seen that $n_L^{+\sigma} > n_L^{-\sigma}$ which means that the time evolution of states on QD1 and QD2 is not related with the time evolution of states in the left lead.

When the energy spacing between the levels for both quantum dots increases i.e. $E_i^{+\sigma} = -1$ eV and $E_i^{-\sigma} = 1$ eV. (see fig.. 7 and 8). There are obvious differences in the values of occupation numbers and current but no new physical features can be noticed.

In figs.(9 to 12), the frequency of the electromagnetic field is increased, $\hbar\omega = 1.5$ eV, this increasing makes the occupation numbers oscillate for more time. In all these figures, it is obvious that at each time when $n_1^{\pm\sigma}$ is maximum, $n_2^{\pm\sigma}$ is minimum and vice versa.

According to fig. 5, one can report the values of the occupation numbers and the spin accumulation on the quantum dots at certain time (see table (5)). These results give physical notes about the tunneling process of the electron with spin up or / and with spin down. At certain time, it is noticed that:

1- $(n_i^{+\sigma} + n_i^{-\sigma}) \leq 1$ for each quantum dots.
2- $\sum_\sigma \sum_{i=1}^{2} n_i^\sigma \leq 2$
3- $n_i^{-\sigma} > n_i^{+\sigma}$ for i=1, 2 as $V_{i\alpha}^{+\sigma} > V_{i\alpha}^{-\sigma}$.
4- At each time, the tunneling process happens for electron with spin up and electron with spin down because the two spin channels are available.

We get also use of fig. 9 to introduce table (6) where $\hbar\omega = 1.5$ eV. All the above mentioned physical notes that are reported for table (5) are also correct for table (6), but as the frequency of the electromagnetic field increases (keeping in mind the other parameters of the electromagnetic field are fixed at the same amplitudes) all the occupation numbers are decreasing. Which means that the tunneling process, for the electron with certain spin, is assisted by increasing the electromagnetic field frequency.

For the same parameters the case of $V_{i\alpha}^{-\sigma} > V_{i\alpha}^{+\sigma}$ and $V_{12}^{-\sigma} > V_{12}^{+\sigma}$ is also investigated (see Tables (7) and (8)). All the above mentioned physical notes are correct for these table with $n_i^{+\sigma} > n_i^{-\sigma}$ for i=1,2 as $V_{i\alpha}^{-\sigma} > V_{i\alpha}^{+\sigma}$ and $V_{12}^{-\sigma} > V_{12}^{+\sigma}$.

In Tables ((5) – (8)) the spin accumulation is also calculated which varies with time, but their values at t=600 a.u. will be highlighted. According to these Tables one can conclude that the type of the accumulated spin is determined by the values of spin – dependent coupling interaction but the accumulated spin is assisted by the fields frequency.

In order to investigate the role of the bias voltage in spin transport in the presence of the fields effect, the occupation number and the spin currents are calculated where $\mu_L = \mu_R = 0.0$ eV with $\hbar\omega = 0.1$ eV (see figs. ((13) and (14))) and $\hbar\omega = 1.5$ eV (see figs.(15) and (16))). By comparing these figures with figs. (1,2,5,6) respectively, one can report the following:

1- The electromagnetic fields parameters effects are dominant in determining the electronic and transport properties of the device.
2- The occupation numbers $n_L^{\pm\sigma}$ on the left lead show higher values than that when $\mu_L = -\mu_R = 2$ eV for both values of $\hbar\omega$.

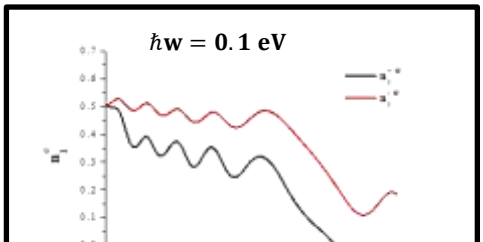

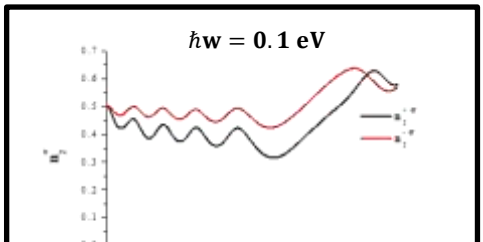

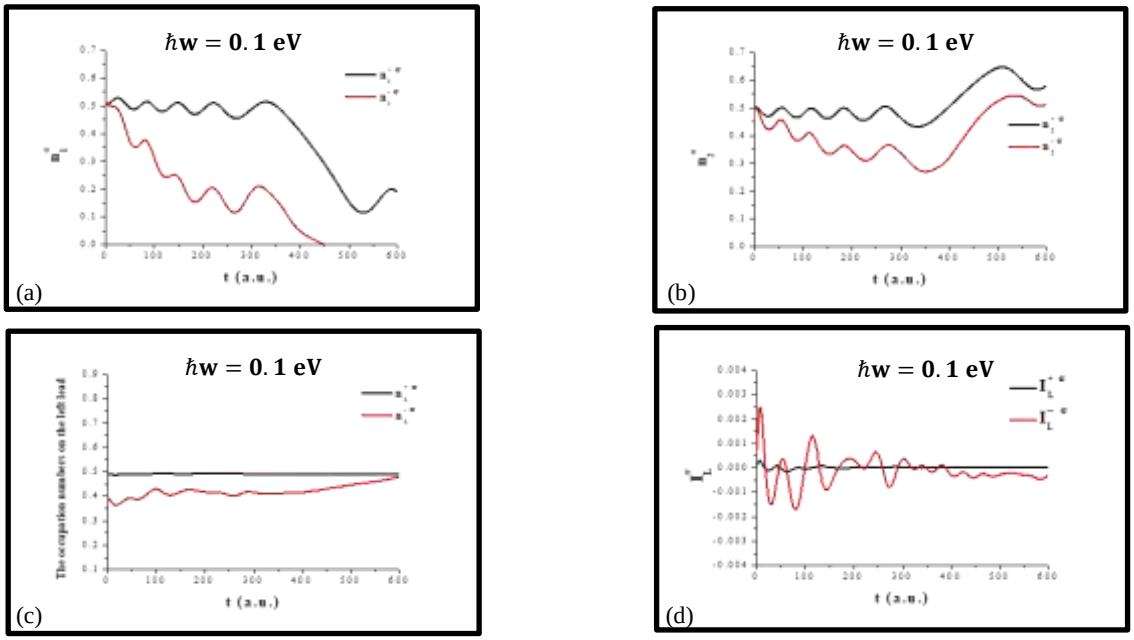

Fig. 6: The occupation numbers of (a) main quantum dot (QD1), (b) side quantum dot (QD2), (c) the left lead and (d) the current flowed from the left lead as a function of time , when

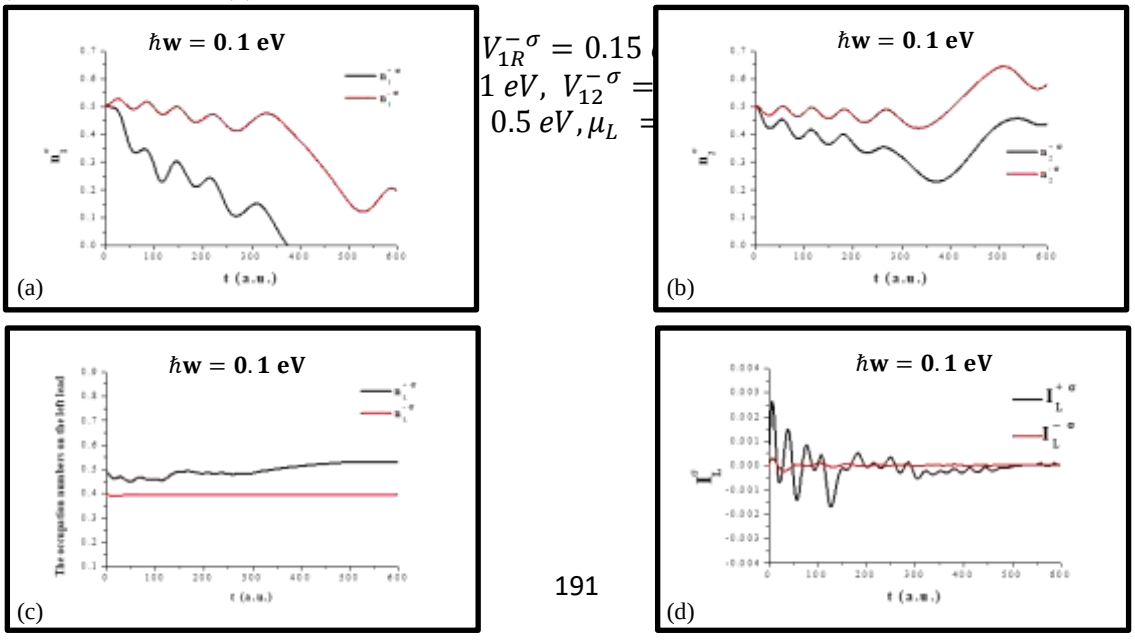

$V_{1R}^{-\sigma} = 0.15$
$1\ eV,\ V_{12}^{-\sigma} =$
$0.5\ eV, \mu_L =$

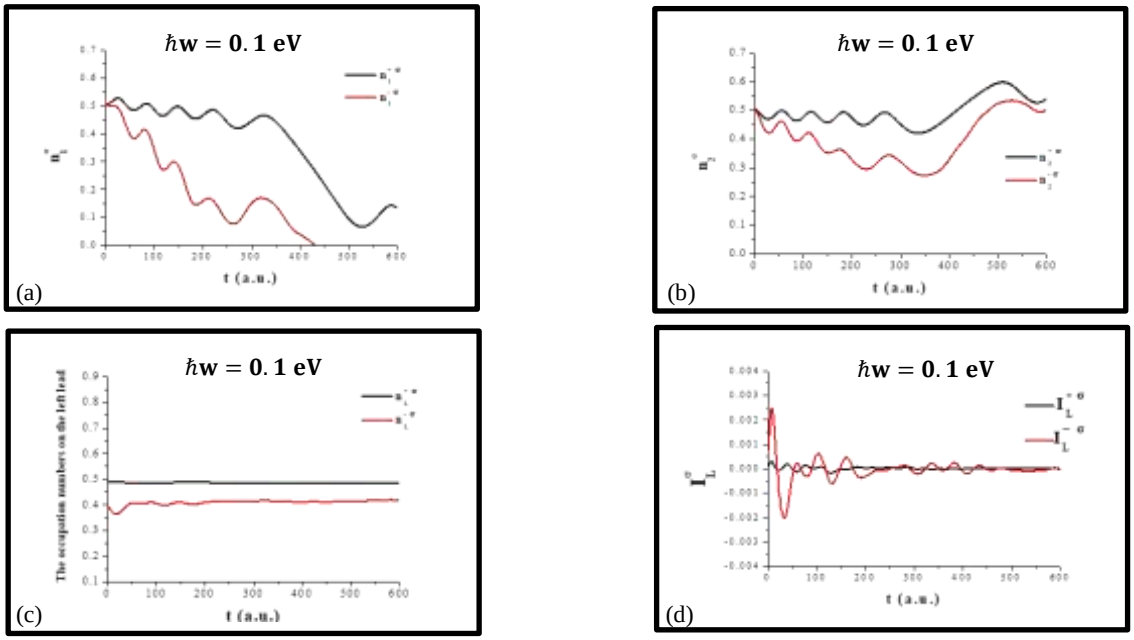

Fig.8 : The occupation numbers of (a) main quantum dot (QD1), (b) side quantum dot (QD2), (c) the left lead and (d) the current flowed from the left lead as a function of time, when

$$V_{1L}^{\sigma} = V_{1R}^{\sigma} = 0.05\ eV,\ V_{1L}^{-\sigma} = V_{1R}^{-\sigma} = 0.15\ eV, \Delta_1 = 4\ eV\ , \Delta_2 = 1\ eV\ ,\ \Delta_L = 3\ eV\ ,\ \Delta_R = 0\ eV, V_{12}^{+\sigma} = V_{21}^{+\sigma} = 0.1\ eV,\ V_{12}^{-\sigma} = V_{21}^{-\sigma} = 0.2\ eV$$

$$E_1^{+\sigma} = E_2^{+\sigma} = -1\ eV,\ E_1^{-\sigma} = E_2^{-\sigma} = 1\ eV, \mu_L = 2\ eV, \mu_R = -2\ eV$$

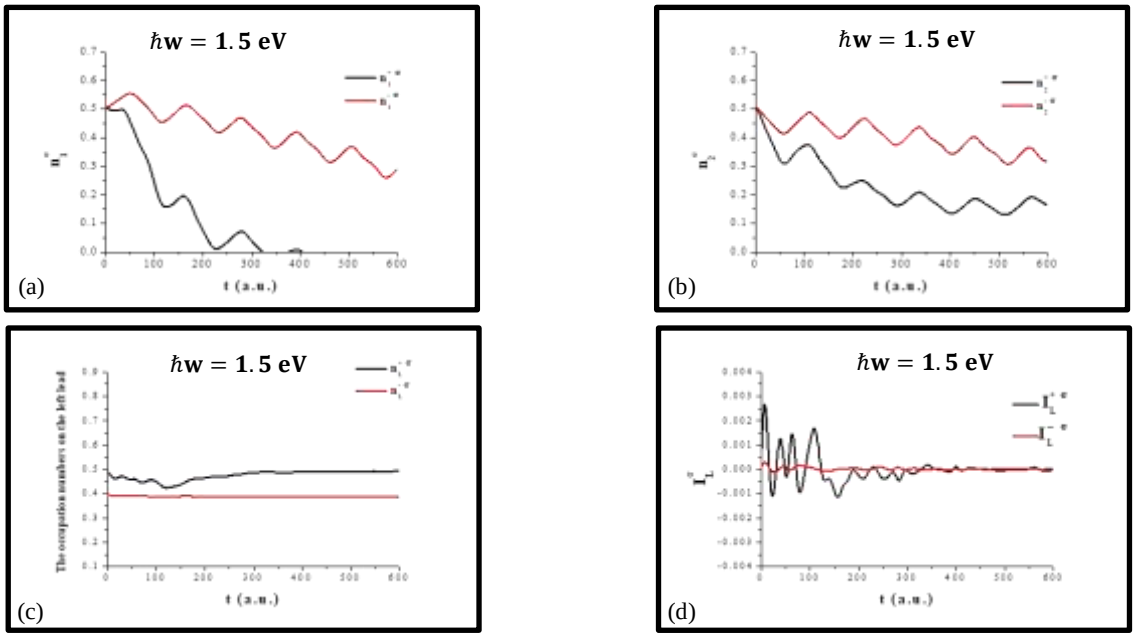

Fig.9: The occupation numbers of (a) main quantum dot (QD1), (b) side quantum dot (QD2), (c) the left lead and (d) the current flowed from the left lead as a function of time , when

$V_{1L}^{\sigma} = V_{1R}^{\sigma} = 0.15\ eV,\ V_{1L}^{-\sigma} = V_{1R}^{-\sigma} = 0.05\ eV, \Delta_1 = 4\ eV, \Delta_2 = 1\ eV,\ \Delta_L = 3\ eV, \Delta_R = 0\ eV, V_{12}^{+\sigma} = V_{21}^{+\sigma} = 0.2\ eV,\ V_{12}^{-\sigma} = V_{21}^{-\sigma} = 0.1\ eV,$

$E_1^{+\sigma} = E_2^{+\sigma} = -0.5\ eV,\ E_1^{-\sigma} = E_2^{-\sigma} = 0.5\ eV, \mu_L = 2\ eV,\ \mu_R = -2\ eV$

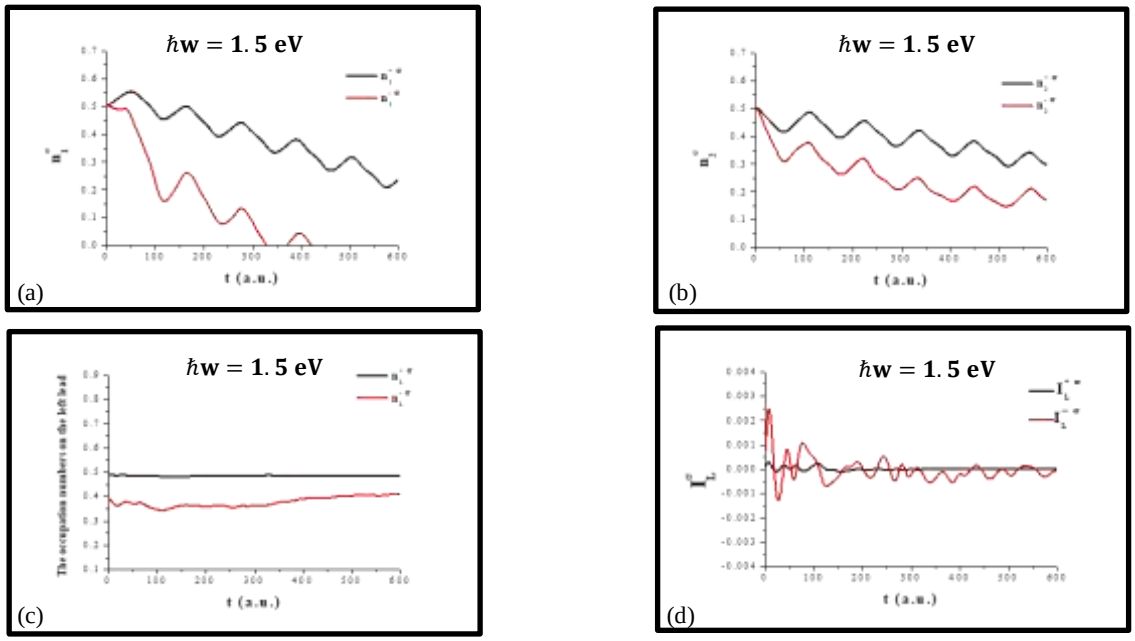

Fig. 10: The occupation numbers of (a) main quantum dot (QD1), (b) side quantum dot (QD2), (c) the left lead and (d) the current flowed from the left lead as a function of time , when

$V_{1L}^{\sigma} = V_{1R}^{\sigma} = 0.05\ eV,\ V_{1L}^{-\sigma} = V_{1R}^{-\sigma} = 0.15\ eV, \Delta_1 = 4\ eV, \Delta_2 = 1\ eV,\ \Delta_L = 3\ eV,\ \Delta_R = 0\ eV, V_{12}^{+\sigma} = V_{21}^{+\sigma} = 0.1\ eV \quad V_{12}^{-\sigma} = V_{21}^{-\sigma} = 0.2\ eV$

$E_1^{+\sigma} = E_2^{+\sigma} = -0.5eV,\ E_1^{-\sigma} = E_2^{-\sigma} = 0.5\ eV. \mu_L = 2\ eV,\ \mu_R = -2\ eV$

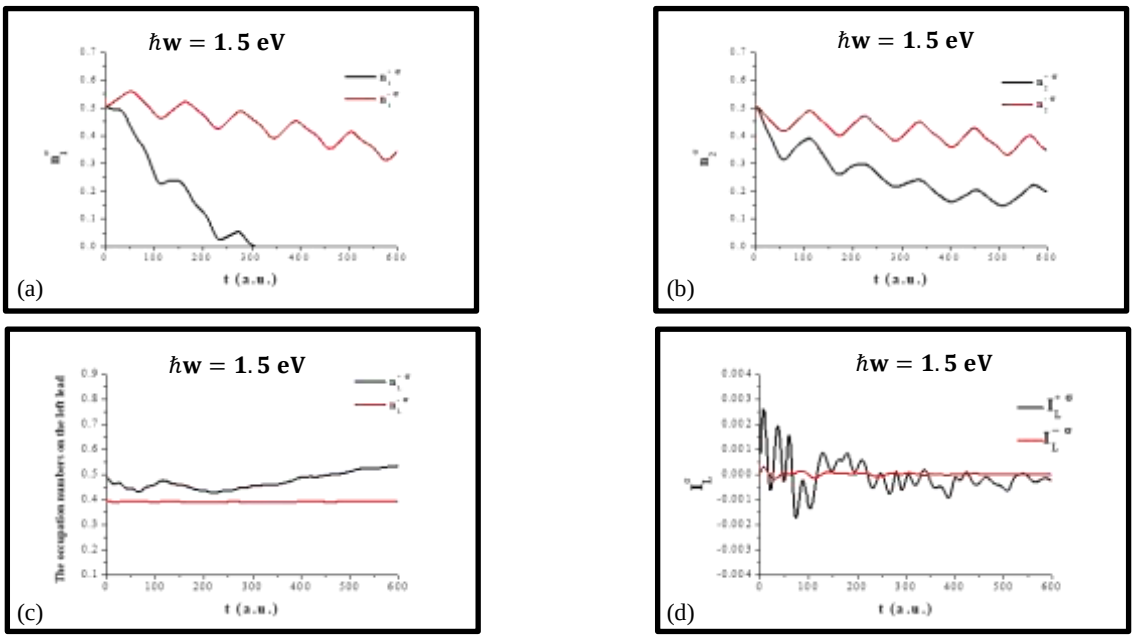

Fig. 11: The occupation numbers of (a) main quantum dot (QD1), (b) side quantum dot (QD2), (c) the left lead and (d) the current flowed from the left lead as a function of time, when

$$V_{1L}^{\sigma} = V_{1R}^{\sigma} = 0.15\ eV, V_{1L}^{-\sigma} = V_{1R}^{-\sigma} = 0.05\ eV, \Delta_1 = 4\ eV\ , \Delta_2 = 1eV,\ \Delta_L = 3\ eV,\ \Delta_R = 0\ eV, V_{12}^{+\sigma} = V_{21}^{+\sigma} = 0.2\ eV,\ V_{12}^{-\sigma} = V_{21}^{-\sigma} = 0.1\ eV$$

$$E_1^{+\sigma} = E_2^{+\sigma} = -1\ eV,\ E_1^{-\sigma} = E_2^{-\sigma} = 1\ eV, \mu_L\ = 2\ eV,\ \mu_R\ = -2\ eV$$

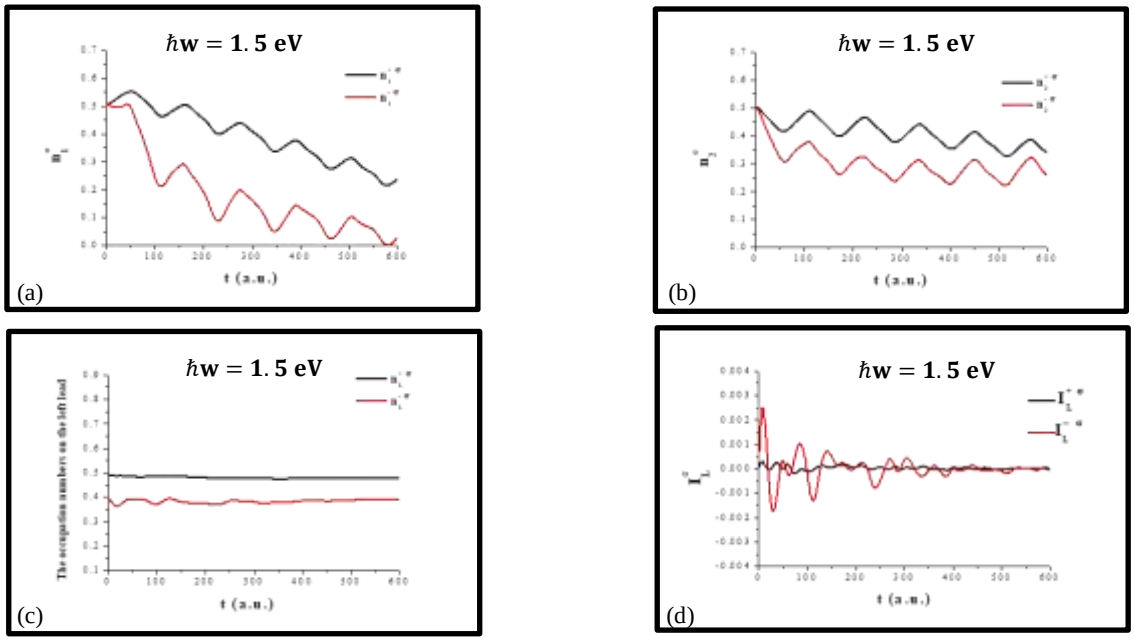

Fig. 12: The occupation numbers of (a) main quantum dot (QD1), (b) side quantum dot (QD2), (c) the left lead and (d) the current flowed from the left lead as a function of time , when

$$V_{1L}^{\sigma} = V_{1R}^{\sigma} = 0.05\ eV,\ V_{1L}^{-\sigma} = V_{1R}^{-\sigma} = 0.15\ eV, \Delta_1 = 4\ eV\ , \Delta_2 = 1\ eV,\ \Delta_L = 3\ eV\ , \Delta_R = 0\ eV, V_{12}^{+\sigma} = V_{21}^{+\sigma} = 0.1\ eV,\ V_{12}^{-\sigma} = V_{21}^{-\sigma} = 0.2\ eV$$

$$E_1^{+\sigma} = E_2^{+\sigma} = -1\ eV,\ E_1^{-\sigma} = E_2^{-\sigma} = 1\ eV, \mu_L\ = 2\ eV,\ \mu_R\ = -2\ eV$$

Table (5): The occupation numbers and spin accumulation on the quantum dots at different times for bulk ScC leads with $\hbar\omega = 0.1\ eV, V_{1L}^{+\sigma} = V_{1R}^{+\sigma} = 0.15\ eV, V_{1L}^{-\sigma} = V_{1R}^{-\sigma} = 0.05\ eV, V_{12}^{+\sigma} = V_{21}^{+\sigma} = 0.2\ eV, V_{12}^{-\sigma} = V_{21}^{-\sigma} = 0.1\ eV,$ $E_1^{+\sigma} = E_2^{+\sigma} = -0.5\ eV,\ E_1^{-\sigma} = E_2^{-\sigma} = 0.5\ eV, \mu_L = 2\ eV, \mu_R = -2\ eV, \Delta_1 = 4\ eV,\ \Delta_2 = 1\ eV,\ \ \Delta_L = 3\ eV\ and\ \Delta_R = 0\ eV$

t (a.u.)	$n_1^{+\sigma}$	$n_1^{-\sigma}$	As1	$n_2^{+\sigma}$	$n_2^{-\sigma}$	As2
100	0.35358	0.49388	-0.14031	0.40040	0.47413	-0.07373
200	0.31747	0.45478	-0.13731	0.40114	0.47221	-0.07107
300	0.30358	0.45953	-0.15595	0.37131	0.45755	-0.08624
400	0.13255	0.38119	-0.24864	0.37895	0.49063	-0.11167
500	0	0.14854	-0.14854	0.53848	0.63340	-0.09492
600	0	0.18356	-0.18356	0.57868	0.56977	-0.00891

Table (6): The occupation numbers and spin accumulation on the quantum dots at different times for bulk ScC leads with $\hbar\omega = 1.5\ eV, V_{1L}^{+\sigma} = V_{1R}^{+\sigma} = 0.15\ eV, V_{1L}^{-\sigma} = V_{1R}^{-\sigma} = 0.05\ eV, V_{12}^{+\sigma} = V_{21}^{+\sigma} = 0.2\ eV, V_{12}^{-\sigma} = V_{21}^{-\sigma} = 0.1\ eV,$ $E_1^{+\sigma} = E_2^{+\sigma} = -0.5\ eV, E_1^{-\sigma} = E_2^{-\sigma} = 0.5\ eV, \mu_L = 2\ eV, \mu_R = -2\ eV, \Delta_1 = 4\ eV,\ \Delta_2 = 1\ eV,\ \ \Delta_L = 3\ eV\ and\ \Delta_R = 0\ eV.$

t (a.u.)	$n_1^{+\sigma}$	$n_1^{-\sigma}$	As1	$n_2^{+\sigma}$	$n_2^{-\sigma}$	As2
100	0.25061	0.47944	-0.22882	0.37003	0.47504	-0.10501
200	0.08005	0.46848	-0.3884	0.23771	0.43357	-0.19586
300	0.04097	0.44014	-0.39917	0.16565	0.38249	-0.21685
400	0.00515	0.41335	-0.4082	0.13516	0.34411	-0.20895
500	0	0.36480	-0.36480	0.13791	0.33320	-0.19529
600	0	0.28791	-0.28791	0.16455	0.31410	-0.14955

Table (7): The occupation numbers and spin accumulation on the quantum dots at different times for bulk ScC leads with $\hbar\omega = 0.1\ eV, V_{1L}^{+\sigma} = V_{1R}^{+\sigma} = 0.05\ eV, V_{1L}^{-\sigma} = V_{1R}^{-\sigma} = 0.15\ eV, V_{12}^{+\sigma} = V_{21}^{+\sigma} = 0.1\ eV, V_{12}^{-\sigma} = V_{21}^{-\sigma} = 0.2\ eV, E_1^{+\sigma} = E_2^{+\sigma} = -0.5\ eV, E_1^{-\sigma} = E_2^{-\sigma} = 0.5\ eV, \mu_L = 2\ eV, \mu_R = -2\ eV, \Delta_1 = 4\ eV,\ \Delta_2 = 1\ eV,\ \Delta_L = 3\ eV$ *and* $\Delta_R = 0\ eV$

t (a.u.)	$n_1^{+\sigma}$	$n_1^{-\sigma}$	As1	$n_2^{+\sigma}$	$n_2^{-\sigma}$	As2
100	0.49811	0.31909	0.17902	0.47522	0.39083	0.0844
200	0.48317	0.17283	0.31034	0.48149	0.34685	0.13463
300	0.48602	0.18949	0.29653	0.46514	0.33909	0.12605
400	0.40825	0.04940	0.35885	0.50276	0.31920	0.18356
500	0.15564	0	0.15564	0.64174	0.52160	0.12014
600	0.19008	0	0.19008	0.57730	0.51089	0.06641

Table (8): The occupation numbers and spin accumulation on the quantum dots at different times for bulk ScC leads with $\hbar\omega = 1.5\ eV, V_{1L}^{+\sigma} = V_{1R}^{+\sigma} = 0.05\ eV, V_{1L}^{-\sigma} = V_{1R}^{-\sigma} = 0.15\ eV, V_{12}^{+\sigma} = V_{21}^{+\sigma} = 0.1\ eV, V_{12}^{-\sigma} = V_{21}^{-\sigma} = 0.2\ eV, E_1^{+\sigma} = E_2^{+\sigma} = -0.5\ eV, E_1^{-\sigma} = E_2^{-\sigma} = 0.5\ eV, \mu_L = 2\ eV, \mu_R = -2\ eV, \Delta_1 = 4\ eV,\ \Delta_2 = 1\ eV,\ \Delta_L = 3\ eV$ *and* $\Delta_R = 0\ eV$.

t (a.u.)	$n_1^{+\sigma}$	$n_1^{-\sigma}$	As1	$n_2^{+\sigma}$	$n_2^{-\sigma}$	As2
100	0.48106	0.23813	0.24294	0.47507	0.37024	0.10484
200	0.44622	0.17731	0.26891	0.42599	0.29176	0.13423
300	0.40916	0.08676	0.3224	0.37138	0.21047	0.16091
400	0.37265	0.04266	0.32999	0.33159	0.16905	0.16253
500	0.31538	0	0.31538	0.31791	0.15784	0.16007
600	0.23561	0	0.23561	0.29736	0.16882	0.12854

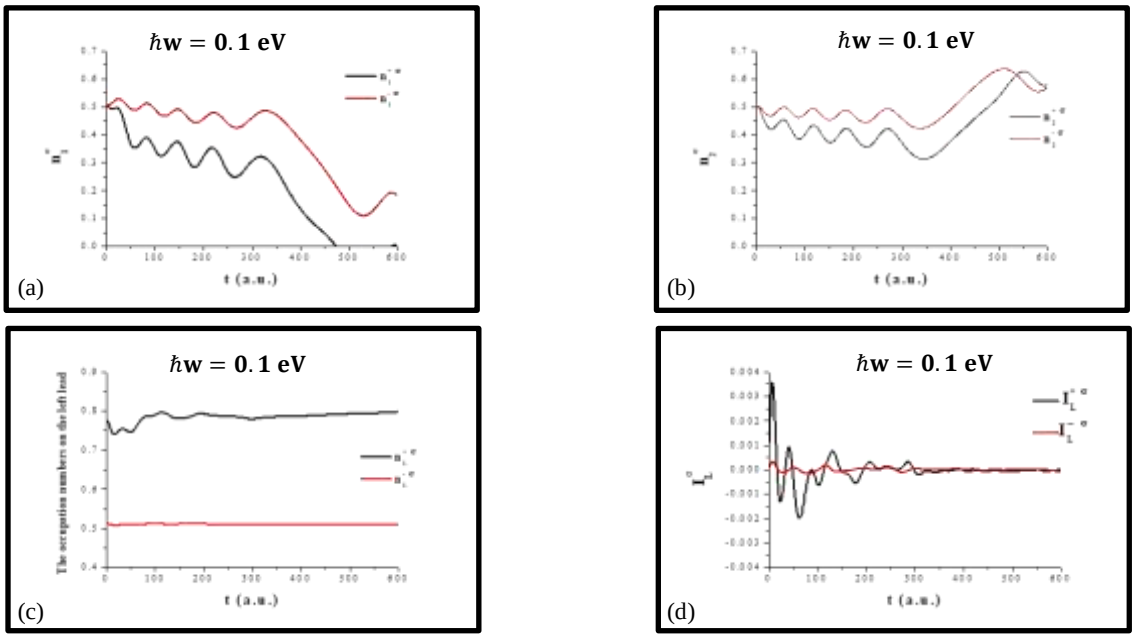

Fig. 13The occupation numbers of (a) main quantum dot (QD1), (b) side quantum dot (QD2), (c) the left lead and (d) the current flowed from the left lead as a function of time , when

$$V_{1L}^{\sigma} = V_{1R}^{\sigma} = 0.15\ eV,\ V_{1L}^{-\sigma} = V_{1R}^{-\sigma} = 0.05\ eV, \Delta_1 = 4\ eV\ , \Delta_2 = 1\ eV,\ \Delta_L = 3\ eV,\ \Delta_R = 0\ eV, V_{12}^{+\sigma} = V_{21}^{+\sigma} = 0.2\ eV,\ V_{12}^{-\sigma} = V_{21}^{-\sigma} = 0.1\ eV$$

$$E_1^{+\sigma} = E_2^{+\sigma} = -0.5\ eV, E_1^{-\sigma} = E_2^{-\sigma} = 0.5\ eV, \mu_L\ = 0.0\ eV,\ \mu_R\ = 0.0\ eV$$

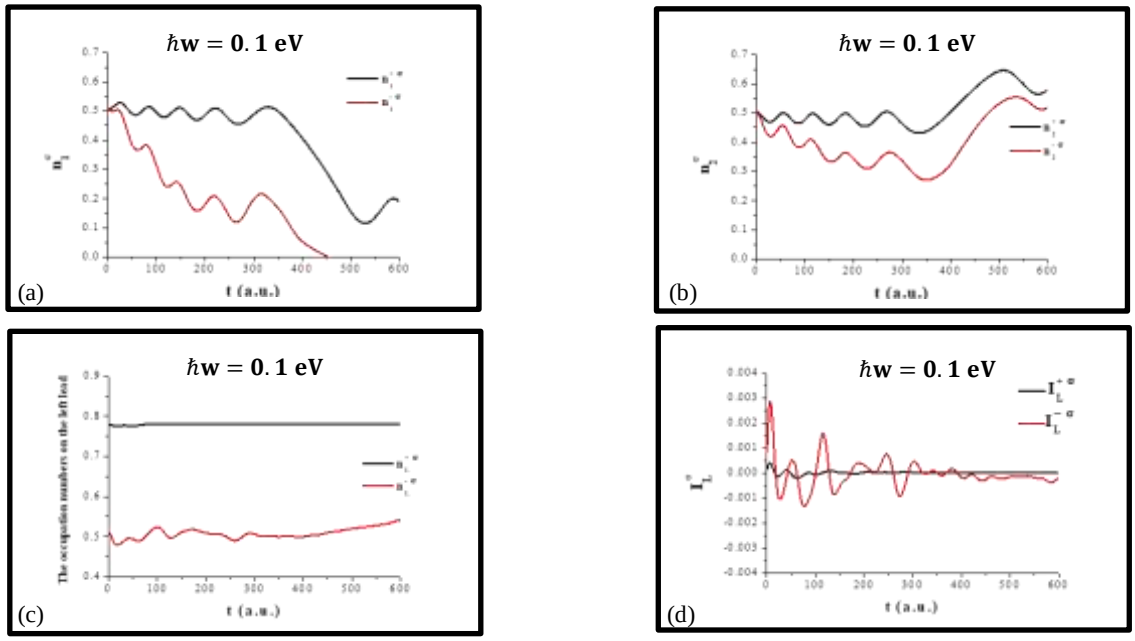

Fig. 14 :The occupation numbers of (a) main quantum dot (QD1), (b) side quantum dot (QD2), (c) the left lead and (d) the current flowed from the left lead as a function of time , when

$$V_{1L}^{\sigma} = V_{1R}^{\sigma} = 0.05\ eV\ , V_{1L}^{-\sigma} = V_{1R}^{-\sigma} = 0.15\ eV, \Delta_1 = 4\ eV\ \ , \Delta_2 = 1\ eV,\ \Delta_L = 3\ eV\ \ ,\ \ \Delta_R = 0\ eV, V_{12}^{+\sigma} = V_{21}^{+\sigma} = 0.1\ eV, V_{12}^{-\sigma} = V_{21}^{-\sigma} = 0.2\ eV$$

$$E_1^{+\sigma} = E_2^{+\sigma} = -0.5\ eV,\ E_1^{-\sigma} = E_2^{-\sigma} = 0.5\ eV, \mu_L\ = 0.0\ eV,\ \mu_R\ = 0.0\ eV$$

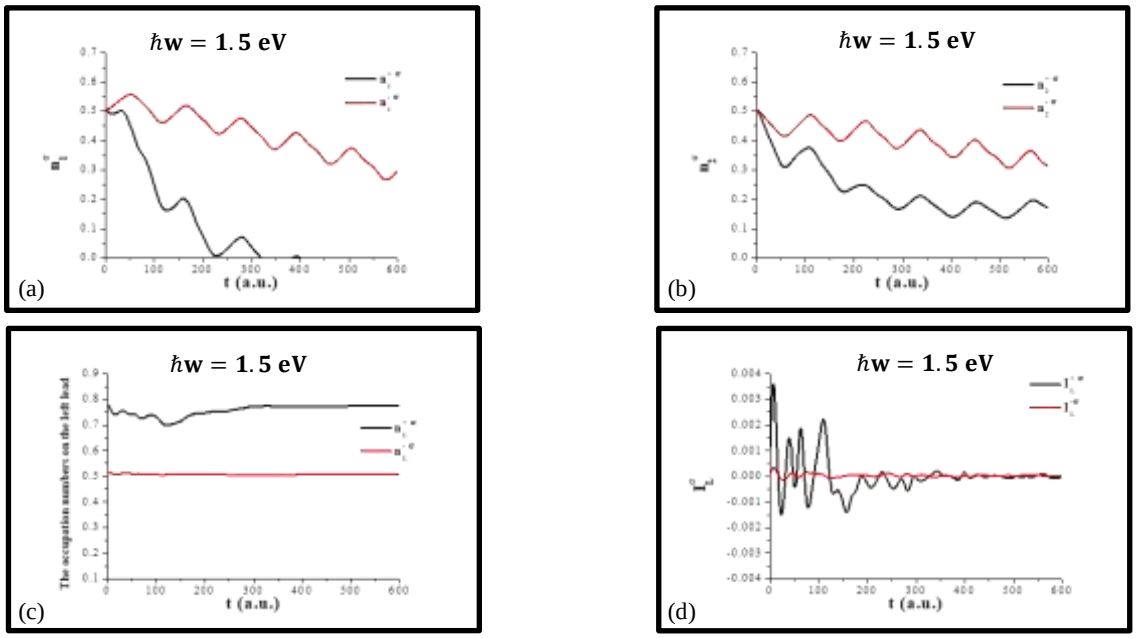

Fig. 15 : The occupation numbers of (a) main quantum dot (QD1), (b) side quantum dot (QD2), (c) the left lead and (d) the current flowed from the left lead as a function of time , when

$$V_{1L}^{\sigma} = V_{1R}^{\sigma} = 0.15\ eV, V_{1L}^{-\sigma} = V_{1R}^{-\sigma} = 0.05\ eV, \Delta_1 = 4\ eV\ , \Delta_2 = 1\ eV,\ \Delta_L = 3\ eV\ ,$$
$$\Delta_R = 0\ eV, V_{12}^{+\sigma} = V_{21}^{+\sigma} = 0.2\ eV,\ V_{12}^{-\sigma} = V_{21}^{-\sigma} = 0.1\ eV$$

$$E_1^{+\sigma} = E_2^{+\sigma} = -0.5\ eV,\ E_1^{-\sigma} = E_2^{-\sigma} = 0.5\ eV, \mu_L\ = 0.0\ eV, \mu_R\ = 0.0\ eV$$

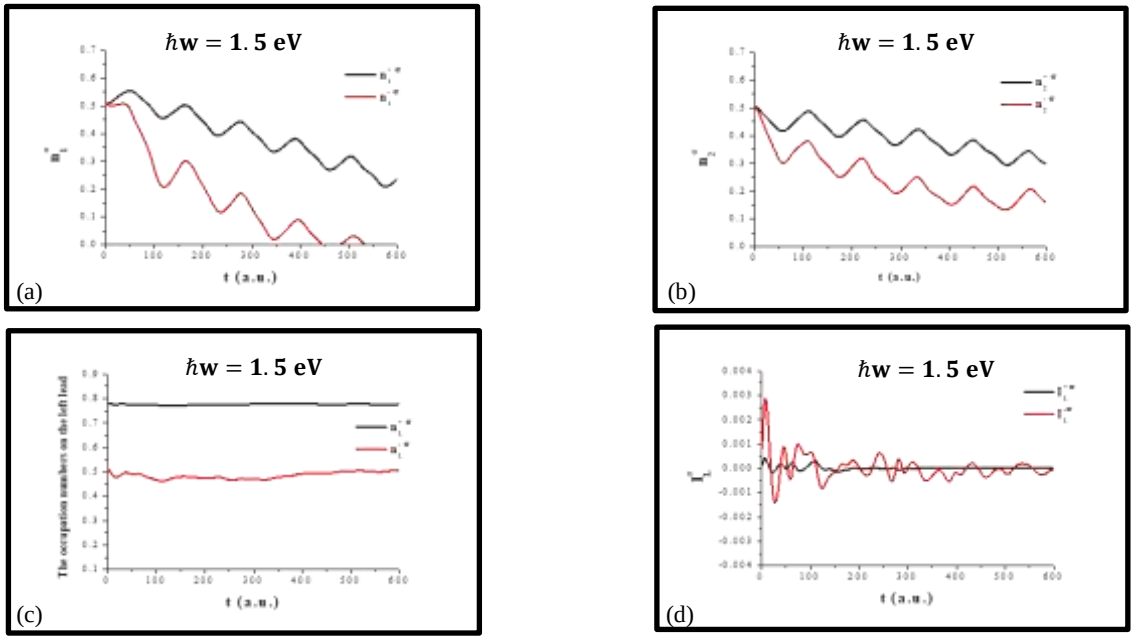

Fig. 16: The occupation numbers of (a) main quantum dot (QD1), (b) side quantum dot (QD2), (c) the left lead and (d) the current flowed from the left lead as a function of time , when

$$V_{1L}^{\sigma} = V_{1R}^{\sigma} = 0.05\ eV,\ V_{1L}^{-\sigma} = V_{1R}^{-\sigma} = 0.15\ eV, \Delta_1 = 4\ eV\ , \Delta_2 = 1\ eV,\ \Delta_L =$$
$$3\ eV\ ,\ \ \Delta_R = 0\ eV, V_{12}^{+\sigma} = V_{21}^{+\sigma} = 0.1\ eV,\ V_{12}^{-\sigma} = V_{21}^{-\sigma} = 0.2\ eV$$

$$E_1^{+\sigma} = E_2^{+\sigma} = -0.5\ eV, E_1^{-\sigma} = E_2^{-\sigma} = 0.5\ eV, \mu_L\ = 0.0\ eV, \mu_R\ = 0.0\ eV$$

5- Conclusions

In our study, the symmetry of the system is broken due to the electronic properties of the device, the bias voltage and the asymmetric of the fields amplitudes. Furthermore, the device is electrically controlled throughout many parameters, namely the position of the quantum dots energy levels and the spin dependent density of states of the (half – metallic) leads. This certainly is visible in all our calculations. Moreover, in order to investigate the imprint of the leads electronic properties on the time dependent spin transport through the device considered in our study, (FPLAPW) method is used to examine the structural, magnetic, and electronic characteristics of the bulk ZB ScC. This study has proven that the bulk ZB ScC is HM ferromagnets at an equilibrium lattice constant (0.5121 nm). In addition, in concern to the spin dependent interdot coupling interaction inequalities in the case of biased system, our results do not contradict with the physical explanation about the time evolution of the spin up and spin down states. With increasing the Zeeman splitting, obvious differences in the values of occupation numbers and current is seen but no new physical features concern to the time evolution of the spin states can be noticed. Besides that increasing of the frequency of the fields makes the occupation numbers oscillate for more time. The spin accumulation calculations give physical notes about the tunneling process of the electrons with spin up or spin down. At each time, the tunneling process occurs for spin up electron and spin down electron because both spin channels are available. As the frequency of the electromagnetic fields increases, the spin accumulation on both quantum dots is assisted. While the type of accumulated spin is determined by the spin dependent interdot coupling interaction. Also, when the system is unbiased, the electromagnetic fields parameters effects are dominant in determining the electronic properties and then the transport properties of the device. The occupation numbers on left lead show higher values than that for the biased system for both values of frequency. This model calculation can be also exploited to study the time dependent spin transport properties for the T-shaped double quantum dots not beyond the wide band approximation.

Finally, we expect that our results are helpful in exploiting the role of electronic coupling interactions (in addition to the assisted field) in spintronics, such as exploiting the spin – filter devices and the quantum computing devices.

6- REFRENCES

[1] J. Y. Bai, Z. L. He and S. B. Yang, Acta Phys. Sin. 63, 017303 (2014).

[2] Z. L. He and T. Q. Lü, Phys. Lett. A 376, 2501 (2012).

[3] Y. X. Li, H. Y. Choi and H. W. Lee, Phys. Lett. A 372, 2073 (2008).

[4] Musa Kadhim Shamer, " Electron Transport through a Quantum Dot : Thermoelectric Effects and Correlation Effects in Kondo and Non-Kondo Regimes ", Ph.D. Thesis, Basrah University, Basrah, (2012).

[5] Reman Jamal Jasm," Theoretical Study in the Thermospin Effects for the Quantum Dot in a Magnetic Field ", M.Sc. Thesis, Basrah University, Basrah, (2017).

[6] R. N. Shang, H. O. Li, G. Cao, M. Xiao, T. Tu, H. W. Jiang, G. C. Guo and G. P. Guo, Appl. Phys. Lett. 103, 162109 (2013).

[7] Yi. Guangyu, An. Limin, G. WeiJiang, Wu. Haina and C. Xiaohui, Phys. Lett. A 377, 1127–1133 (2013).

[8] H.B. Heersche, Z. de Groot, J.A. Folk, L.P. Kouwenhoven, H.S.J. van der Zant, A. A. Houck, J. Labaziewicz and I.L. Chuang, Phys. Rev. Lett. 96, 017205 (2006).

[9] Hui Pan and Yinghui Zhao, J. Phys. : Condends. Matt. 21, 265501 (2009).

[10] I. Tifrea, M. Crisan and I. Grosu, Eur. Phys. J. B 79, 455 (2011).

[11] H. Pan and Y.H.Zhao, Eur. Phys. J. B 70, 185 (2009).

[12] R. Zitko, Phys. Rev. B 81, 115316 (2010).

[13] W.G. van der Wiel, S. De Franceschi, J.M. Elzerman, T. Fujisawa,S. Tarucha and K.P. Kouwenhoven, Rev.Mod. Phys. 75, 1 (2003).

[14] D. S. Golubev, M. S. Kalenkov and A. D. Zaikin, Phys. Rev. Lett. 103, 067006 (2009).

[15] Nordberg. Charge sensing in enhancement mode double top gated metal-oxide-semiconductor quantum dots. Applied Physics Letters 95, 202102 (2009).

[16] J. Baranski and T. Domanski, Phys. Rev. B 85, 205451(2012).

[17] A. Fujiwara, Y. Takahashi and K. Murase, Phys. Rev. Lett.78, 1532 (1997).

[18] He. Zelong,n, Bai. Jiyuan, Cui. Lian, Li. Qiang, Han. Guihua and Z. Binlin, Physica B 477, 64–69(2015).

[19] J. Barna´s and I. Weymann, J. Phys.: Condens. Matt. 20, 423202 (2008).

[20] T. Kwapinski and R. Taranko, science direct, Physica E 18, 402 – 411(2003)

[21] R. Taranko, E. Taranko and M. Wiertel, Acta Phys. POL. A 103, 483 (2003).

[22] R. Taranko, T.Kwapinski and E.Taranko, Phys. Rev. B 69, 165306 (2004).

[23] Thikra S. Dh. Al-Naser," Charge Exchange Process in the Scattering of Irons off Adsorbate – covered Surface ", M.Sc. Thesis, Basrah University, Basrah, (2003).

[24] Jenan M. Al- Mukh, " charge Transfer Between Atom (Ion) and Metal Surfaces ", Ph.D. Thesis, Basrah University, Basrah, (1997).

[25] A. S. Davydov, "Quantum Mechanics" Second Russain Edition Published by Nauka, Moscow, (1973).

[26] T. Kwapinski, R. Taranko and E. Taranko, Phys. Rev. B 66, 035315 (2002).

[27] R. Taranko, T. Kwapinski, and E. Taranko, Phy. Rev. B 69, 165306 (2004).

[28] O. Entin Wohlman, Amnon Aharony and Y.Levinson, Phys.Rev. B 65, 195411 (2002).

[29] T. Mii, K. Makoshi and H. Ueba, Surf. Sci. 493, 575-584 (2001).

[30] H. M. Obeed." Time-dependent Electron Transport through a Quantum Dot Assisted by Electromagnetic Field: In the Presence and Absence of the Nonresonant Channal", "M.Sc. Thesis, Basrah University, Basrah, (2014).

[31] J. J. Deng, J. H. Zhao, J. F. Bi, Z. C. Niu, F. H. Yamg, X. G. Wu, and H. Z. Zheng, J. Appl. Phys. 99, 093902 (2006).

[32] K. Ozdogan, E. Sasioglu, and I. Galanakis, J. Magn. Magn. Mater. 322, 46 (2010).

[33] J. M. Khalaf Al-zyadi," Surface half-metallicity in several binary/ternary compounds", Ph.D. Thesis, Huazhong University of Science and Technology, (2013).

[34] G. Y. Gao, K. L. Yao, E. Sasioglu, L. M. Sandratskii, Z. L. Liu and J. L. Jiang, Phys. Rev. B 75, 174442 (2007).

[35] B. G. Liu, Lecture Notes in Physics, Vol. 676, pp. 267–291 (Springer, Berlin, (2005)).

نقل البرم المعتمد على الزمن خلال نظام نقطتين كميتين على هيئة T موضوعتين بين قطبين (الحجم ScC نصف المعدني)

ماجد عبدالله ناطق و جنان مجيد المخ وجبار منصور خلف

قسم الفيزياء، كلية التربية للعلوم الصرفة، جامعة البصرة

الخلاصة

للأهمية العملية و النظرية لنقل البرم المعتمد على الزمن خلال تراكيب النقاط الكمية، تمت دراسة وتحليل نقل البرم المدعوم مجال كهرو مغناطيسي خلال نقطتين كميتين بهيئة T موضوعتين بين قطبين غير اعتياديين. الهاملتونين المعتمد على الزمن الذي يصف الجهاز يتبع اسلوب الترابط المتين في أخذ تفاعلات الاقتران المعتمدة على البرم بنظر الاعتبار بين اجزاء النظام. لقد انجزت المعالجة النظرية باستخدام اسلوب مؤثر الزمن – النمو، حيث اشتقت معدلات الحركة بتمثيل التفاعل لعناصر مصفوفة مؤثر الزمن – النمو. معادلات الحركة التفاضلية – التكاملية ال 32 لكلا البرم تم حلها عددياً باستخدام طريقة رانج – كوتا من الرتبة السادسة، اذ تم التحقق من الخطأ في كل خطوة زمنية. تم التوصل الى الحسابات المعتمدة على الطاقة بأعتبار كثافة الحالات للأقطاب غير الاعتيادية. بينما استخدم التقريب الاديباتيكي لمعالجة تأثيرات مميزات المجال الكهرومغناطيسي الخارجي (التردد و السعة) نظرياً.

في ما يخص بالأقطاب الغير اعتيادية، استغلت طريقة (FPLAPW) هذه الطريقة تعتمد على استخدام نظرية دالة الكثافة (DFT) لفحص المميزات التركيبية و المغناطيسية و الالكترونية للصلد ZB ScC. هذه الدراسة برهنت أن الصلد ZB ScC هو نصف معدني الفيرومغناطيسية عند ثابت الشبيكة المتزن (0.512 nm). الهدف الاساسي لدراستنا، هو فحص تأثيرات المجال الكهرومغناطيسي على جهاز النقطتين الكميتين بهيئة T ، لذلك كل الخصائص الالكترونية للنظام بالإضافة الى معاملات المجال الكهرومغناطيسي المأخوذ بنظر الاعتبار في معالجتنا. تم تحليل و تفسير دور تردد المجال و تفاعل الاقتران المعتمدة على البرم للاقطاب الصلد ScC.

الكلمات المفتاحية: الألكترونيات البرمية، التركيب النانو المغناطيسي، كثافة الحالات لنصف المعدن، نقل البرم المعتمد على الزمن، تقنية مؤثر النمو الزمني.